

## Distribution Agreement

In presenting this thesis as a partial fulfillment of the requirements for a degree from Emory University, I hereby grant to Emory University and its agents the non-exclusive license to archive, make accessible, and display my thesis in whole or in part in all forms of media, now or hereafter now, including display on the World Wide Web. I understand that I may select some access restrictions as part of the online submission of this thesis. I retain all ownership rights to the copyright of the thesis. I also retain the right to use in future works (such as articles or books) all or part of this thesis.

Ashley Hodges

April 10, 2012

Synthesis, characterization, and biological stabilities of gold(III) di-2-pyridyl  
and *sec*-butyl-phenanthroline complexes

by

Ashley Hodges

Dr. Cora MacBeth  
Adviser

Department of Chemistry

Dr. Cora MacBeth  
Adviser

Dr. Patricia Marsteller  
Committee Member

Dr. Jeremy Weaver  
Committee Member

April 10, 2012

Synthesis, characterization, and biological stabilities of gold(III) di-2-pyridyl  
and *sec*-butyl-phenanthroline complexes

By

Ashley Hodges

Dr. Cora Macbeth

Adviser

An abstract of  
a thesis submitted to the Faculty of Emory College of Arts and Sciences  
of Emory University in partial fulfillment  
of the requirements of the degree of Bachelor of Arts  
with Honors

Department of Chemistry

2012

## Abstract

### Synthesis, characterization, and biological stabilities of gold(III) di-2-pyridyl and *sec*-butyl-phenanthroline complexes

By Ashley Hodges

In an effort to develop novel gold-based chemotherapies, gold(III) coordination complexes possessing a series of dipyridyl ligands were targeted as synthetic products. It was found that dipyridyl ligands linked by different groups exhibited varying coordination to gold(III). Dipyridyl sulfide (DPS) exhibited bidentate binding to gold(III), and formed a complex ion with a gold tetrachloride counter ion  $\{[(DPS)AuCl_2]AuCl_4$ ; compound **3** $\}$ ; dipyridyl oxide (DPO) formed a neutral monodentate coordination complex with gold(III)  $\{[(DPO)(AuCl_3)]$ ; compound **4** $\}$ ; and attempts to make gold(III) complexes with dipyridyl ketone (DPK) were unsuccessful, as a complex ion possessing the protonated ligand and a gold tetrachloride anion was isolated  $\{[DPK-H]AuCl_4$ ; compound **5** $\}$ . Compounds **3-5** were structurally characterized using X-ray crystallography, which confirmed the different coordination environments about the gold(III) metal centers. Compound **4** was further characterized by  $^1H$  NMR and UV-vis spectroscopy, and its DNA binding and buffer stability were determined. Compound **4** displayed minimal DNA binding, but was found to have poor stability in the presence of the biological reductant reduced glutathione (GSH).

After completing studies of the dipyridyl ligands, differentially alkylated phenanthroline ligands were synthesized and complexed with gold. These ligands included 5,6-dimethyl-2,9-disecbutyl-1,10-phenanthroline, 4-methyl-2,9-disecbutyl-1,10-phenanthroline, 4,5,6,7-tetramethyl-2,9-disecbutyl-1,10-phenanthroline, and 5-methyl-2,9-disecbutyl-1,10-phenanthroline. The gold complexes of 5,6-dimethyl-2,9-disecbutyl-1,10-phenanthroline and 4-methyl-2,9-disecbutyl-1,10-phenanthroline were chosen for biological stability studies, including

buffer stability, glutathione buffer stability, and ascorbic acid stability. Their in vitro DNA binding was also probed. Both of these complexes demonstrated stability in slightly basic buffer and GSH buffer. They did not appear as stable in the presence of ascorbic acid, and also exhibited in vitro DNA binding. Despite the DNA binding and the lack of stability in ascorbic acid, these compounds appear promising for potential use in biological systems.

Synthesis, characterization, and biological stabilities of gold(III) di-2-pyridyl  
and *sec*-butyl-phenanthroline complexes

By

Ashley Hodges

Dr. Cora Macbeth

Adviser

An abstract of  
a thesis submitted to the Faculty of Emory College of Arts and Sciences  
of Emory University in partial fulfillment  
of the requirements of the degree of Bachelor of Arts  
with Honors

Department of Chemistry

2012

## **Acknowledgements**

The research conducted during this project was made possible by funding from the Oxford College Research Scholars Program, the Pierce Institute for Leadership and Community Engagement, and the Howard Hughes Medical Institute Grant. In addition to this funding, I would also like to acknowledge the following programs and departments for their support in this research: the Oxford College Department of Chemistry, the Summer Undergraduate Program at Emory, the Emory University Department of Chemistry, and the Scholarly Inquiry and Research at Emory program.

I would also like to thank Suk C. Lee for her role in guidance and help with the synthesis of the gold(III) di-2-pyridyl complexes. In addition, I would like to thank Chinar Sanghvi for her role in introducing me to the gold project and all of the laboratory techniques necessary to conduct this research. Dylan Jones also provided valuable guidance and support for this project.

The most crucial acknowledgements I would like to make are to thank my research mentors, Dr. Cora Macbeth and Dr. Jack Eichler. Both of these mentors were crucial in introducing me to the exciting world of research, and helping me through the problem-solving skills necessary to conducting this project. Without their support, this research would not have been possible.

## Table of Contents

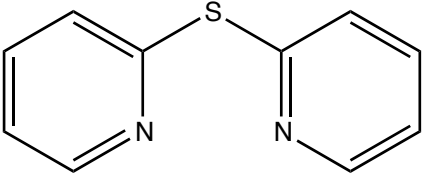
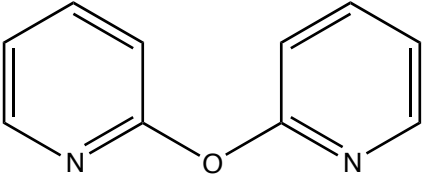
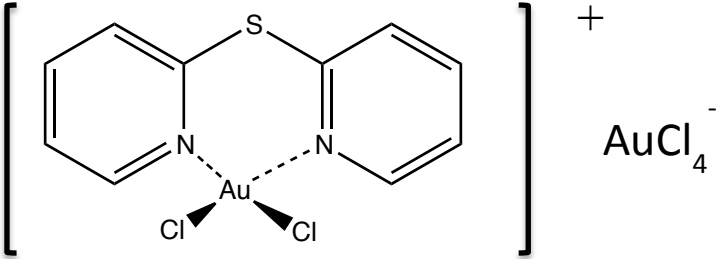
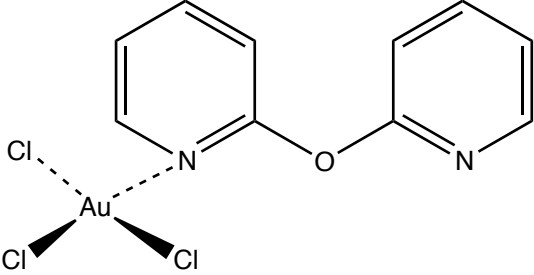
<b>Introduction.....</b>	<b>5</b>
<b>Experimental.....</b>	<b>13</b>
<i>General Experimental Procedures .....</i>	<b>13</b>
<i>Synthesis of dipyridyl sulfide (1).....</i>	<b>13</b>
<i>Synthesis of dipyridyl oxide (2).....</i>	<b>13</b>
<i>Synthesis of gold(III) dipyridyl sulfide (3).....</i>	<b>14</b>
<i>Synthesis of gold(III) dipyridyl oxide (4) .....</i>	<b>14</b>
<i>Synthesis of gold(III) dipyridyl ketone (5).....</i>	<b>15</b>
<i>Synthesis of 5,6-dimethyl-2,9-disecbutyl-1,10-phenanthroline ligand (6).....</i>	<b>15</b>
<i>Synthesis of 5,6-dimethyl-2,9-disecbutyl-1,10-phenanthroline gold (III) complex (7)...</i>	<b>16</b>
<i>Synthesis of 4-dimethyl-2,9-disecbutyl-1,10-phenanthroline ligand (8) .....</i>	<b>16</b>
<i>Synthesis of 4-methyl-2,9-disecbutyl-1,10-phenanthroline gold (III) complex (9) .....</i>	<b>17</b>
<i>Synthesis of 4,5,6,7-tetramethyl-2,9-disecbutyl-1,10-phenanthroline ligand (10) .....</i>	<b>17</b>
<i>Synthesis of 4,5,6,7-tetramethyl-2,9-disecbutyl-1,10-phenanthroline gold (III) (11) ...</i>	<b>18</b>
<i>Synthesis of 5-methyl-2,9-disecbutyl-1,10-phenanthroline ligand (12).....</i>	<b>18</b>
<i>Synthesis of 5-methyl-2,9-disecbutyl-1,10-phenanthroline gold (III) complex (13).....</i>	<b>19</b>
<i>X-ray crystallographic studies.....</i>	<b>19</b>
<i>Buffer Stability studies.....</i>	<b>20</b>
<i>GSH Buffer stability studies – Dipyridyl Ligands.....</i>	<b>20</b>
<i>DNA binding studies- Dipyridyl Ligands.....</i>	<b>20</b>
<i>DNA Binding Studies- Phenanthroline Ligands.....</i>	<b>21</b>
<b>Results and Discussion.....</b>	<b>22</b>
<i>Synthesis .....</i>	<b>22</b>
<i><sup>1</sup>H NMR and UV-vis Spectroscopy.....</i>	<b>23</b>
<i>X-Ray Crystal Structures.....</i>	<b>28</b>
<i>Buffer Stability.....</i>	<b>34</b>
<i>GSH Buffer Stability.....</i>	<b>37</b>
<i>Ascorbic Acid Stability .....</i>	<b>39</b>

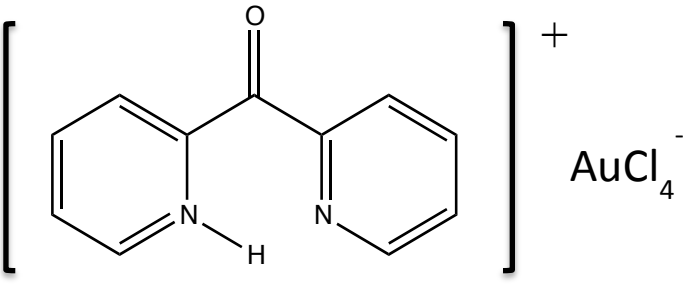
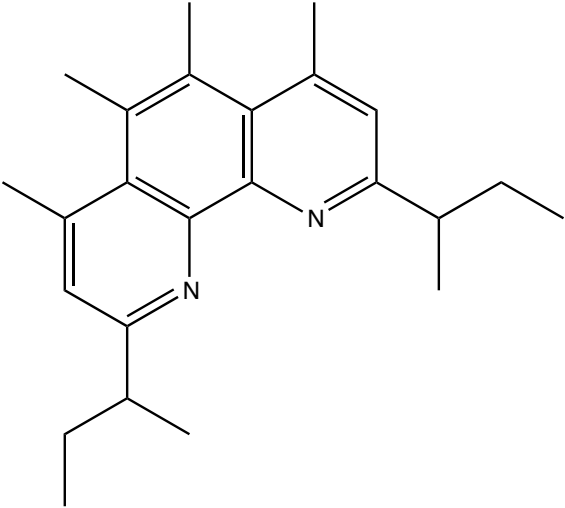
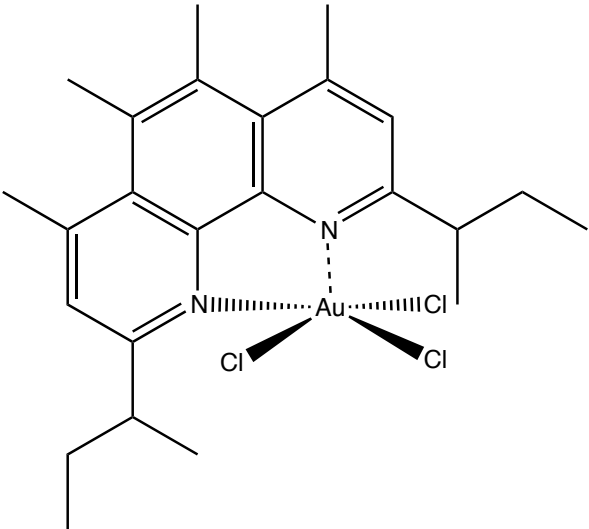


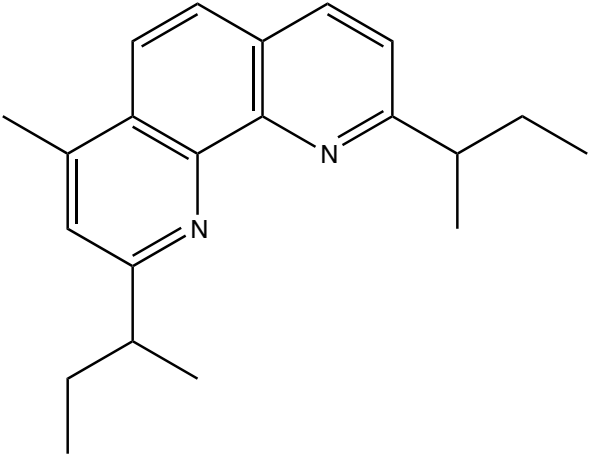
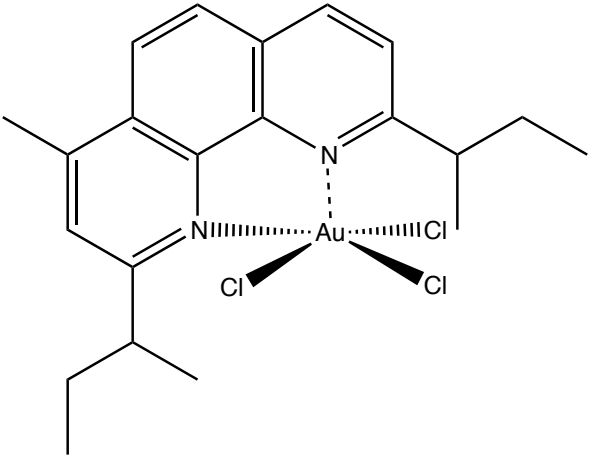
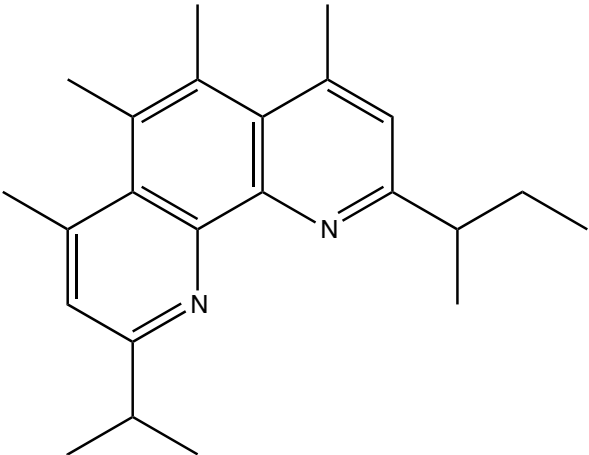
<i>DNA Binding</i> .....	41
<b>Conclusion</b> .....	44
<b>References</b> .....	46
<b>Figures, Tables, and Schemes</b>	
<i>Compound Numbering Legend</i> .....	1
<i>Scheme 1</i> .....	7
<i>Scheme 2</i> .....	9
<i>Scheme 3</i> .....	9
<i>Scheme 4</i> .....	10
<i>Scheme 5</i> .....	10
<i>Scheme 6</i> .....	11
<i>Scheme 7</i> .....	11
<i>Scheme 8</i> .....	12
<i>Scheme 9</i> .....	12
<i>Figure 1</i> .....	25
<i>Figure 2</i> .....	26
<i>Figure 3</i> .....	27
<i>Figure 4</i> .....	30
<i>Figure 5</i> .....	30
<i>Figure 6</i> .....	31
<i>Figure 7</i> .....	32
<i>Figure 8</i> .....	36
<i>Figure 9</i> .....	36
<i>Figure 10</i> .....	38
<i>Figure 11</i> .....	38
<i>Figure 12</i> .....	39
<i>Figure 13</i> .....	40
<i>Figure 14</i> .....	41

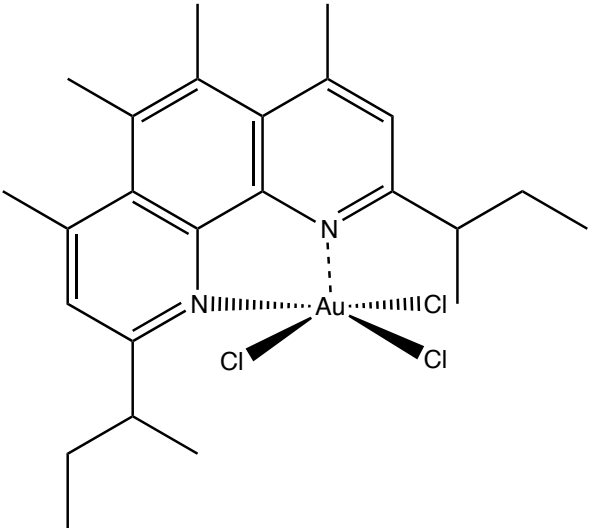
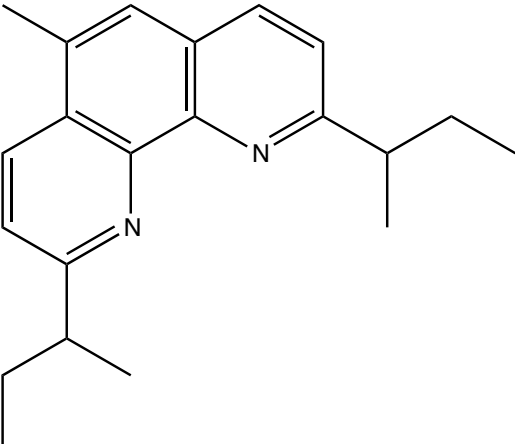
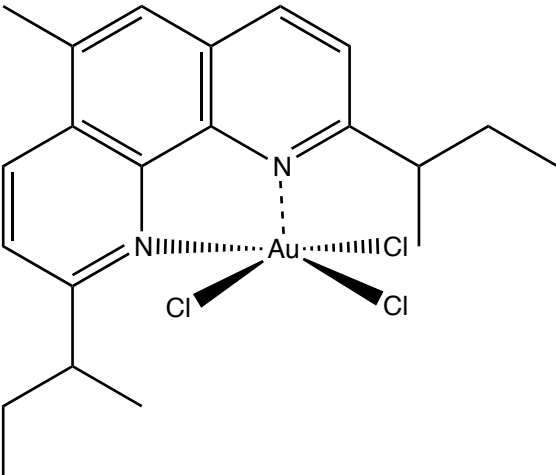
<i>Figure 15</i> .....	<b>42</b>
<i>Figure 16</i> .....	<b>43</b>
<i>Figure 17</i> .....	<b>43</b>
<i>Table 1</i> .....	<b>8</b>
<i>Table 2</i> .....	<b>22</b>
<i>Table 3</i> .....	<b>23</b>
<i>Table 4</i> .....	<b>32</b>
<i>Table 5</i> .....	<b>33</b>
<i>Table 6</i> .....	<b>34</b>

## Compound Numbering Legend

Structure Legend	Compound #
 <p>Chemical structure of 1,2-bis(pyridin-2-yl)ethane-1-thiolate, showing two pyridine rings connected by a sulfur atom at the 2-position of each ring.</p>	<b>1</b>
 <p>Chemical structure of 1,2-bis(pyridin-2-yl)ethane-1-yl ether, showing two pyridine rings connected by an oxygen atom at the 2-position of each ring.</p>	<b>2</b>
 <p>Chemical structure of a gold complex. The central gold atom (Au) is coordinated to two chlorine atoms (Cl) and two nitrogen atoms (N) of a bis(pyridin-2-yl)ethane-1-thiolate ligand. The complex is shown in brackets with a plus sign, and the counterion is <math>\text{AuCl}_4^-</math>.</p>	<b>3</b>
 <p>Chemical structure of a gold complex. The central gold atom (Au) is coordinated to two chlorine atoms (Cl) and two nitrogen atoms (N) of a bis(pyridin-2-yl)ethane-1-yl ether ligand. The complex is shown with a plus sign, and the counterion is <math>\text{AuCl}_4^-</math>.</p>	<b>4</b>

 <p><math>\left[ \text{Schiff base} \right]^+ + \text{AuCl}_4^-</math></p>	5
	6
	7

 <p>Chemical structure of a bis-imidazole ligand. It consists of two imidazole rings connected at their 2-positions. The left imidazole ring has a methyl group at the 4-position and an isopropyl group at the 5-position. The right imidazole ring has an isopropyl group at the 4-position and a methyl group at the 5-position.</p>	<b>8</b>
 <p>Chemical structure of a bis-imidazole ligand coordinated to a gold atom (Au). The gold atom is coordinated to the N2 atoms of both imidazole rings via dashed lines. Additionally, the gold atom is coordinated to two chlorine atoms (Cl) via solid lines, one shown with a wedge bond and the other with a dash bond.</p>	<b>9</b>
 <p>Chemical structure of a bis-imidazole ligand, identical to the one in row 8. It consists of two imidazole rings connected at their 2-positions. The left imidazole ring has a methyl group at the 4-position and an isopropyl group at the 5-position. The right imidazole ring has an isopropyl group at the 4-position and a methyl group at the 5-position.</p>	<b>10</b>

 <p>Chemical structure 11: A gold(I) complex. The central gold atom (Au) is coordinated to two nitrogen atoms (N) of a bis-imino ligand and two chloride ligands (Cl). The ligand consists of two pyridine rings fused to a central benzene ring, with ethyl and isopropyl substituents. The gold atom is coordinated to the two nitrogen atoms of the imino groups and two chloride ligands.</p>	<b>11</b>
 <p>Chemical structure 12: The bis-imino ligand from structure 11, shown without the gold complex. It consists of two pyridine rings fused to a central benzene ring, with ethyl and isopropyl substituents.</p>	<b>12</b>
 <p>Chemical structure 13: A gold(I) complex, identical to structure 11. The central gold atom (Au) is coordinated to two nitrogen atoms (N) of a bis-imino ligand and two chloride ligands (Cl). The ligand consists of two pyridine rings fused to a central benzene ring, with ethyl and isopropyl substituents. The gold atom is coordinated to the two nitrogen atoms of the imino groups and two chloride ligands.</p>	<b>13</b>

## Introduction

Cancer research is a continuously evolving field. The importance of progressive research towards new anticancer drugs is illustrated by cancer's rank as the second leading cause of death in the United States.<sup>1</sup> Efforts to discover new therapies have resulted in the synthesis of a wide variety of molecular species, including a number of inorganic coordination complexes possessing various metal ions.<sup>2-14</sup> The posterchild for metal-based chemotherapies is the Pt(II)-based compound diaminodichloroplatinum(II), commonly referred to as cisplatin. Cisplatin has been one of the most successful chemotherapies in the last 30 years and has been used to treat numerous types of cancer, including testicular, ovarian, head-neck, and bladder tumors among others.<sup>12</sup> Despite having great utility as a chemotherapy, cisplatin does have drawbacks; only select tumor types are responsive to treatment with cisplatin, tumors often develop resistance to the drug, and cisplatin often results in systemic toxicity.<sup>12</sup> Subsequently, researchers are continually looking for alternatives that might address these limitations.

In this vein, gold-based compounds have long been explored for their anticancer activity. Historically, this was driven by the fact that patients receiving a gold(I) drug for the treatment of rheumatoid arthritis were found to have fewer cancer diagnoses than the general population, and because subsequent studies found that gold(I) compounds inhibited the growth of HeLa cells.<sup>11</sup> Additionally, it was thought that since gold(III) is isoelectronic to platinum(II) and often forms square planar complexes analogous to cisplatin, this class of compounds might also possess significant anti-tumor activity. Unfortunately, gold(I) drugs have not been found to possess significant therapeutic advantages over cisplatin, and gold(III) compounds were shown to be somewhat unstable in biological environments.<sup>8-11</sup>

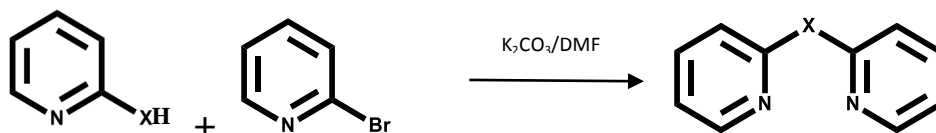
More recent studies have demonstrated that polydentate ligands often enhance the stability of gold(III) complexes in biological environments, and despite the fact gold(III) complexes are often structural analogues to cisplatin, they impart tumor cell death via a different mechanism. Instead of disrupting DNA replication,<sup>14</sup> gold(III) drugs most likely induce apoptosis by disrupting the function of intracellular proteins involved in regulating normal mitochondrial function.<sup>15-17</sup> These findings have led to a resurgence in the development of gold(III)-based chemotherapies, and several classes of compounds, including gold(III) porphyrins, gold(III) dithiocarbamates, and dioxo dinuclear gold(III) complexes possessing polypyridyl ligands, are showing promise as potentially viable chemotherapies.<sup>18-21</sup>

Given the fact that polypyridyl ligands such as phenanthroline and bipyridine have often been used to synthesize potential gold(III) compounds possessing antitumor properties, our group sought to explore the use of dipyriddy moieties as ligands for gold(III) coordination complexes.<sup>22-26</sup> Numerous metal dipyriddy complexes have been previously reported, including silver(I) and copper(II) complexes possessing bidentate dipyriddy sulfide (DPS) ligands,<sup>27,28</sup> platinum(II) complexes with bidentate dipyriddy oxide (DPO) ligands,<sup>29</sup> and platinum(II) metal ions found to form coordination complexes with bidentate dipyriddy ketone (DPK) ligands. However, these classes of ligands have not to date been reported with gold(III). Therefore, we have attempted to make gold(III) complexes with these three classes of dipyriddy ligands, and report herein the different modes of coordination that occur upon reaction with gold(III) (see Scheme 1), as well as the full characterization, DNA binding, and solution stability of the gold(III) complex possessing the DPO ligand (compound **4**).



## Scheme 1

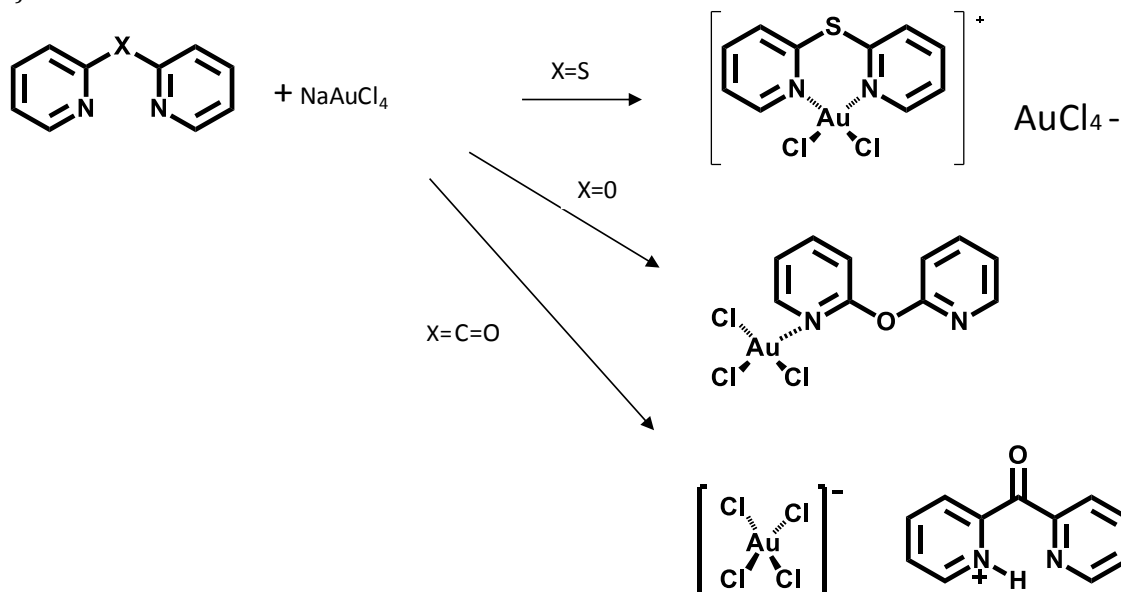
a)



X = S (1) (Journal of the Chemical Society, Perkin II 1976 (pg 1234 - 1238))

X = O (2)

b)



In addition to synthesizing and characterizing the above three classes of dipyridyl ligands, I also synthesized alkylated phenanthroline ligands. Previous work in our laboratory has demonstrated that gold complexes possessing 5,6-dimethylphenanthroline ligand exhibited negligible DNA binding, but were found to undergo immediate reduction to gold(I) in the presence of biological reductants. Our studies also showed that gold complexes possessing 2,9-dimethylphenanthroline ligands were stable in the presence of biological reducing agents, but these complexes were also found to interact with DNA. To maximize the stability and cytotoxicity while minimizing the DNA binding properties of the resulting gold complexes, we

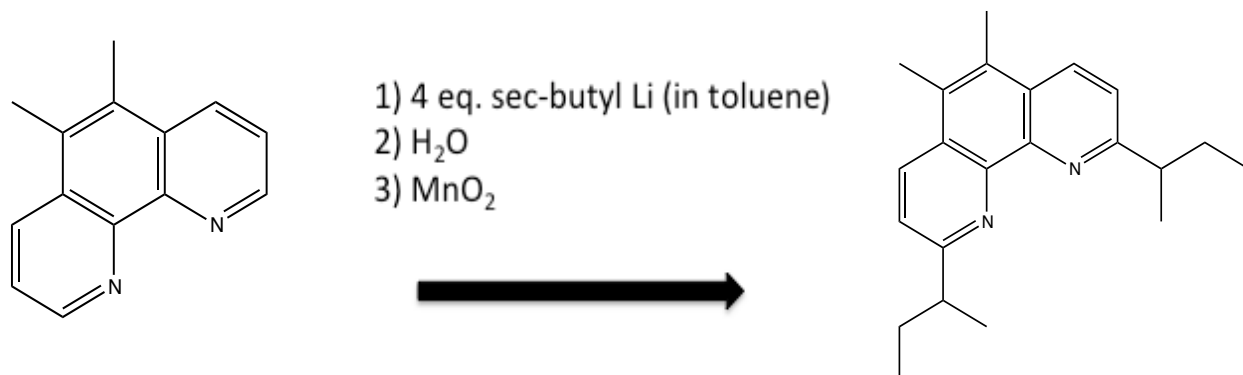
sought to target a new family of 2,9-disubstituted-1,10-phenanthroline ligands. The 2,9-disec-butyl-1,10-phenanthroline ligand demonstrated strong cytotoxicity in vivo when probed against a variety of cancer cell lines from head and neck tumors, including cisplatin-resistant cell lines (as seen in Table 1).<sup>30</sup>

	A549 (L)	886LN (H & N)	Tu212 (H & N)	Tu686 (H & N)	H1703 (L, <i>cis</i> - platin resistant )
<b>sec-butylphen</b>	0.08	0.18	0.07	0.09	0.07
<b>[(sec-butylphen) AuCl<sub>3</sub>]</b>	0.76	1.60	0.34	1.16	0.20
<b>[<sup>n</sup>butylphenH] [AuCl<sub>4</sub>]</b>	0.37	1.13	0.16	0.38	0.09
<b>[(methylbipy) AuCl<sub>3</sub>]</b>	4.36	23.30	12.80	N/A	2.40
<b>cisplatin</b>	2.95	4.80	2.60	2.80	10.85

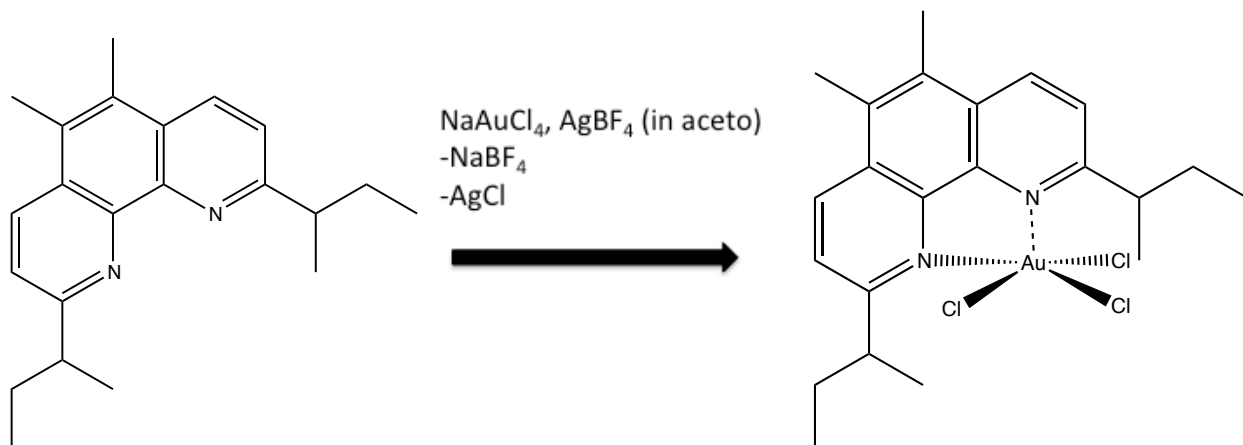
Table 1. IC50 Cytotoxicity Results from Head and Neck Tumor Cell Lines

To begin this segment of my project I synthesized 2,9-disecbutyl-5,6-dimethyl phenanthroline and fully characterized it using various UV-vis, NMR spectroscopy, and X-ray crystallography (Synthesis- See Scheme 2 and 3). The goal of adding the sec-butyl groups to the 5,6-dimethyl-1,10-phenanthroline complex, was to combine the cytotoxicity and low DNA binding of the sec-butyl phenanthroline ligands with the biological stability of the dimethyl-phenanthroline ligands; thus synthesizing a compound that possesses strong cytotoxicity and low DNA binding when probed, as well as favorable biological stability. Because DNA binding is a

non-specific mechanism of attack that attacks both healthy and cancerous cell lines, a more specified mechanism of attack is desirable.<sup>31</sup> Gold(III) is believed to involve the inhibition of TrxR, which induces apoptosis. This could potentially lead to greater selectivity because TrxR is up-regulated in cancer cells versus healthy cell lines.<sup>32</sup>



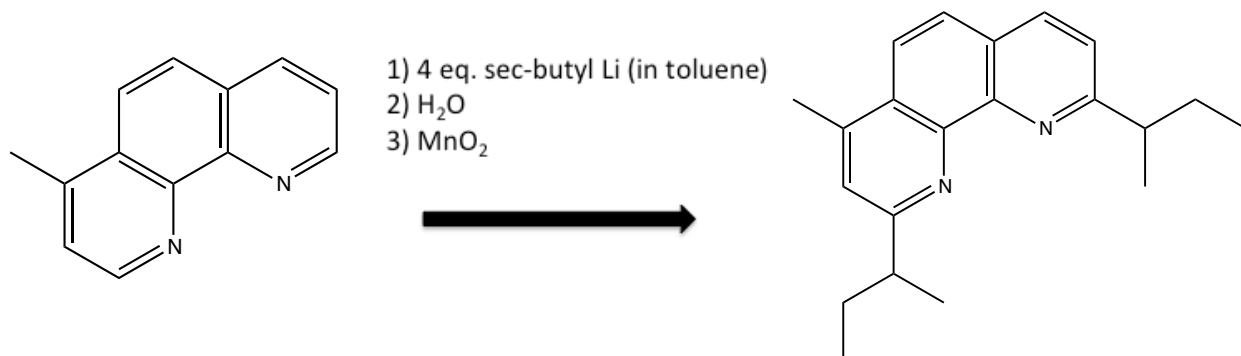
Scheme 2. Synthesis of 2,9-disebutyl-5,6-dimethyl phenanthroline (compound 6)



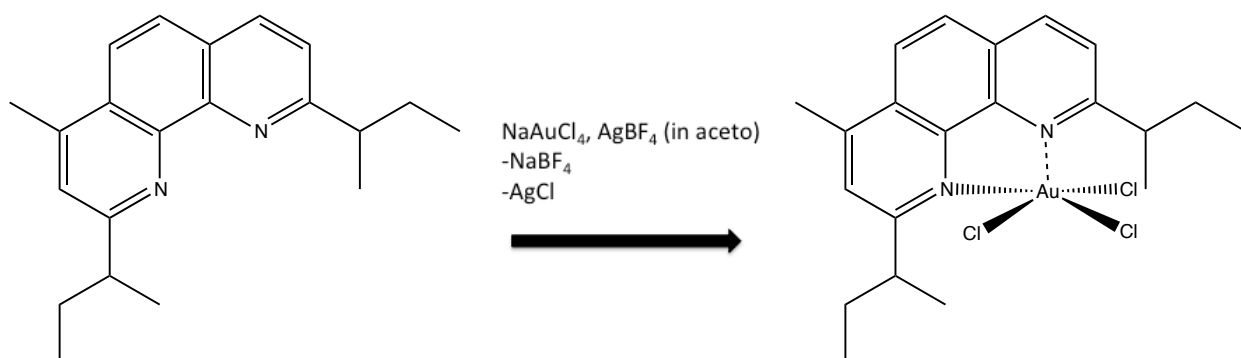
Scheme 3. Synthesis of the 2,9-disebutyl-5,6-dimethyl phenanthroline gold complex (compound 7)

In an effort to determine the effect of subtle changes to the ligand on the electrochemical properties of the resulting gold(III) compound, the gold complexes possessing 2,9-disebutyl-4-methyl phenanthroline, 2,9-disebutyl-5-methyl phenanthroline, and 2,9-disebutyl-4,5,6,7-

tetramethyl phenanthroline were both synthesized and characterized. First, the 2,9-disubstituted-4-methyl phenanthroline ligand and its gold complex were synthesized (See Schemes 4 and 5).



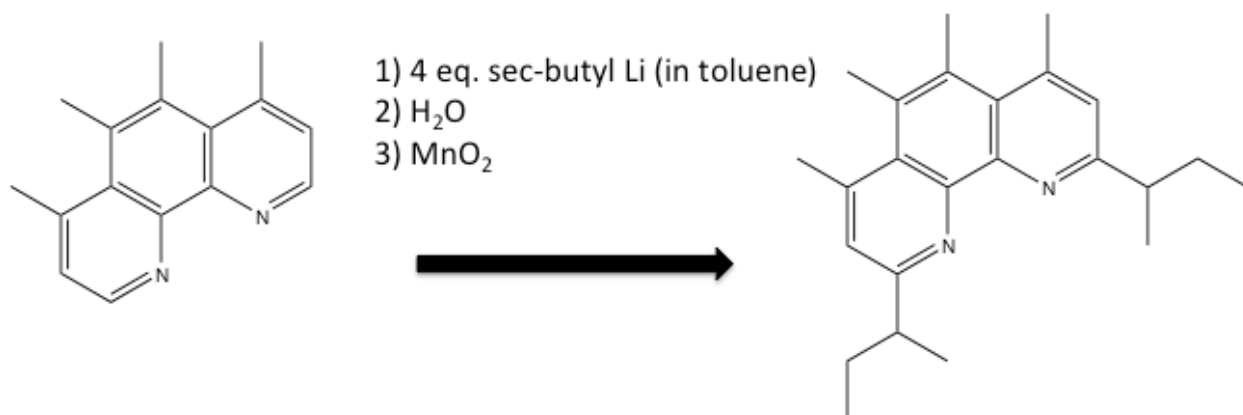
Scheme 4. Synthesis of 2,9-disubstituted-4-methyl phenanthroline (compound **8**)



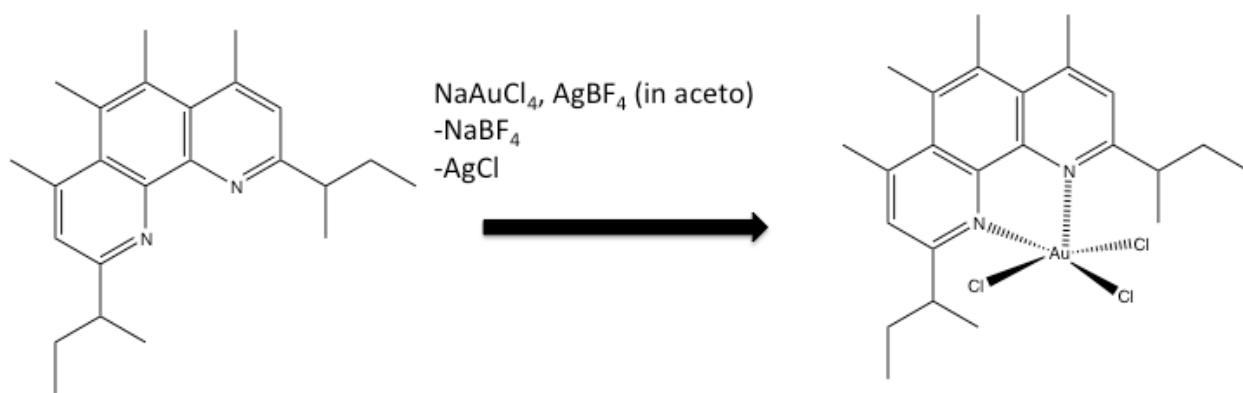
Scheme 5. Synthesis of the 2,9-disubstituted-4-methyl phenanthroline gold complex (compound **9**)

After the synthesis of the 2,9-disubstituted-5,6-dimethyl phenanthroline ligand and the 2,9-disubstituted-4-methyl phenanthroline ligand, and their respective gold complexes, two more ligand complexes were synthesized. These two new ligands were the 4,5,6,7-tetramethyl-2,9-disubstituted-1,10-phenanthroline ligand and the 5-methyl-2,9-disubstituted-1,10-phenanthroline ligand.

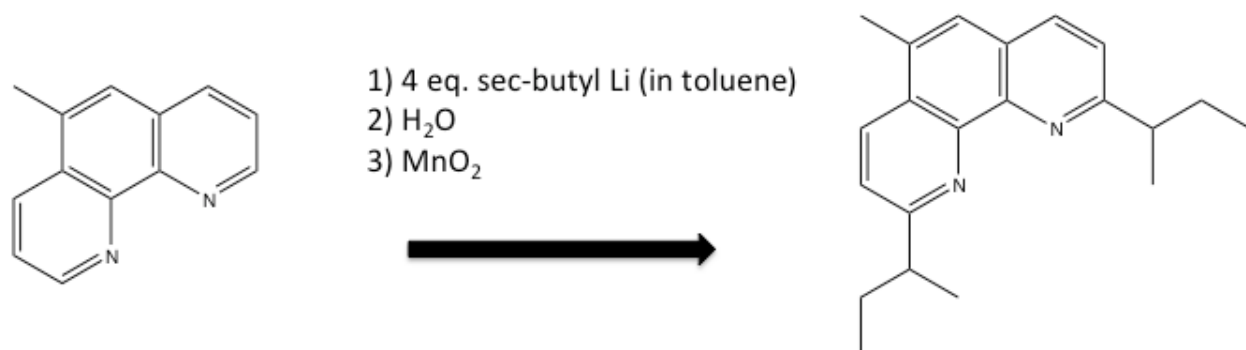
Following these synthesis reactions, both of these ligands were purified using flash column chromatography and then complexed with gold (III). The gold complexes were recrystallized to improve purity.



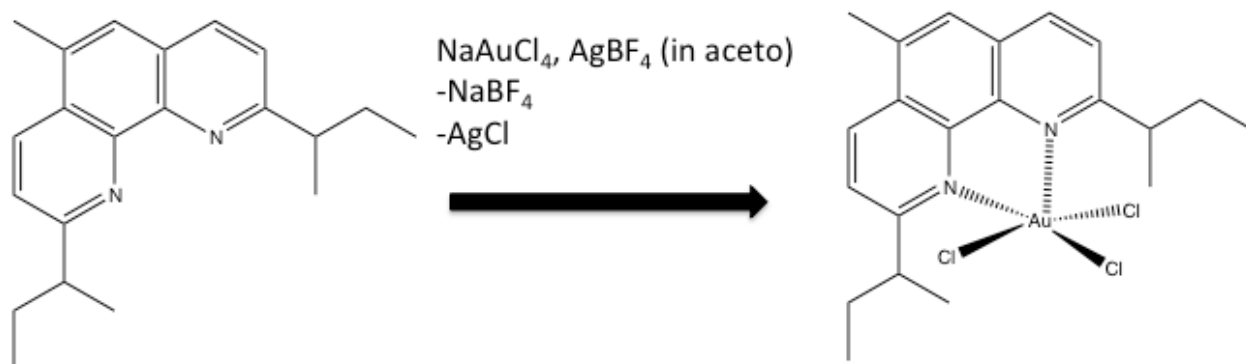
Scheme 6. Synthesis of the 4,5,6,7-tetramethyl-2,9-disebutyl-1,10-phenanthroline ligand (compound **10**)



Scheme 7. Synthesis of the 4,5,6,7-tetramethyl-2,9-disebutyl-1,10-phenanthroline gold complex (compound **11**)



Scheme 8. Synthesis of the 5-methyl-2,9-disecbutyl-1,10-phenanthroline ligand (compound **12**)



Scheme 9. Synthesis of the 5-methyl-2,9-disecbutyl-1,10-phenanthroline gold (III) complex (compound **13**)

## Experimental

### *General Experimental Procedures*

Calf thymus DNA, chloroform, dipyridyl ketone, silver tetrafluoroborate, and sodium tetrachloroaurate were purchased from Sigma-Aldrich, Inc. All reagents were used without further purification, except that the calf thymus DNA was made into a 1 mg/mL stock solution in 10 mM phosphate buffer (pH 7.4, 20 mM NaCl).  $^1\text{H}$  NMR was recorded on a Varian Mercury spectrometer at 300 MHz in  $\text{CDCl}_3$  or  $\text{DMSO-d}_6$ , using the chloroform singlet at 7.20 ppm or DMSO pentet at 2.50 ppm, respectively, as internal references. UV-vis were recorded on a Cary 50 UV-Vis spectrophotometer, and elemental analyses were performed by Atlantic Microlab, Inc.

### *Synthesis of dipyridyl sulfide (1)*

The dipyridyl sulfide ligand was synthesized as previously reported in the literature.<sup>36</sup> The product was purified via Kugelrohr distillation (0.1 torr/150°C).  $^1\text{H}$  NMR ( $\text{CDCl}_3$ , 300 MHz)/ppm: 9.66 (dd, 2H); 9.44 (dd, 2H); 8.41 (dd, 2H); 2.89 (s, 6H).

### *Synthesis of dipyridyl oxide (2)*

1.0 grams of bromo-pyridine (6.33 mmole) was combined with 0.6 grams of hydroxopyridine (6.33 mmole) in DMF (approximately 30 mL) and refluxed overnight. The resulting orange colored solution was filtered and the solvent removed *in vacuo* using a rotary evaporator. The resulting oil was purified via Kugelrohr distillation (0.1 torr/175°C), and then column chromatography (silica, 10% ethyl acetate in hexane). The final yield of **2** was 0.100 g (9.2% yield).  $^1\text{H}$  NMR ( $\text{CDCl}_3$ , 300 MHz)/ppm: 9.66 (dd, 2H); 9.44 (dd, 2H); 8.41 (dd, 2H); 2.89 (s, 6H).

*Synthesis of gold(III) dipyridyl sulfide (3)*

0.211 g of  $\text{NaAuCl}_4 \cdot 2\text{H}_2\text{O}$  was measured and added to 0.100 g of **1** in acetonitrile and refluxed for an hour, and then an acetonitrile solution containing 0.103 g of  $\text{AgBF}_4$  was added and the resulting reaction mixture refluxed overnight. The  $\text{AgCl}$  precipitate was filtered off and acetonitrile was removed by rotary evaporation. The yellow solid synthesized was redissolved in a minimum amount of hot methanol. X-ray quality crystals were obtained by slowly evaporating the methanol. The final yield was 0.075 g, (10% yield). The experiment was repeated with 2 equivalents of  $\text{AgBF}_4$ , with the same resulting product and approximate yield. Elemental analysis ( $\text{C}_{14}\text{H}_{12}\text{N}_2\text{Cl}_2\text{AuBF}_4$ ): experimental (C = 29.47%, H = 2.17%); calculated (C = 29.87%, H = 2.15%).

*Synthesis of gold(III) dipyridyl oxide (4)*

0.100 grams of **2** was dissolved in acetonitrile and added to 0.231 g of  $\text{NaAuCl}_4 \cdot 2\text{H}_2\text{O}$  in acetonitrile and refluxed for an hour, and then an acetonitrile solution containing 0.113 g of  $\text{AgBF}_4$  was added and the resulting reaction mixture was refluxed overnight. The  $\text{AgCl}$  precipitate was filtered off and acetonitrile was removed by rotary evaporation. The yellow solid synthesized was redissolved in a minimum amount of hot methanol. X-ray quality crystals were obtained by slowly evaporating the methanol. The final yield was 0.050 g (18.1%).  $^1\text{H}$  NMR (DMSO- $d_6$ , 300 MHz)/ppm: 9.66 (dd, 2H); 9.44 (dd, 2H); 8.41 (dd, 2H) 2.89 (s, 6H); UV-Vis:  $\lambda_{\text{max}}$  (acetonitrile, 20°C)/nm ( $\epsilon$ ,  $\text{M}^{-1}\text{cm}^{-1}$ ) 240 (49 000 ), 290 (5 200), 315 (shoulder, 13 000), 370 (broad, 2 000); Elemental analysis ( $\text{C}_{14}\text{H}_{12}\text{N}_2\text{Cl}_2\text{AuBF}_4$ ): experimental (C = 29.47%, H = 2.17%); calculated (C = 29.87%, H = 2.15%).



*Synthesis of gold(III) dipyridyl ketone (5)*

0.200 grams of dipyridyl ketone ligand was dissolved in acetonitrile and added to 0.432 g of  $\text{NaAuCl}_4 \cdot 2\text{H}_2\text{O}$  in acetonitrile and refluxed for an hour, and then an acetonitrile solution containing 0.113 g of  $\text{AgBF}_4$  was added and the resulting reaction mixture was refluxed overnight. The  $\text{AgCl}$  precipitate was filtered off and acetonitrile was removed by rotary evaporation. The yellow solid was redissolved in a minimum amount of hot methanol and recrystallized by slow evaporation of solvent. The experiment was attempted with both 1 equivalent and 2 equivalents of  $\text{AgBF}_4$ , but no complex was formed in which the ligand directly coordinated to the gold(III) metal center.

*Synthesis of 5,6-dimethyl-2,9-disecbutyl-1,10-phenanthroline ligand (6)*

0.500 grams of 5,6-dimethyl-1,10-phenanthroline ligand was dissolved in anhydrous toluene under a nitrogen flow. An excess of sec-butyl lithium, 5 milliliters, was added drop-wise to the toluene reaction mixture. During this overnight reaction period, the round bottom flask was kept in ice water. After this overnight reaction, the reaction mixture was removed from the vessel, and the inorganic impurities and side products were removed using a liquid-liquid extraction. This extraction was performed twice with 50 milliliters of deionized water. The water layer was discarded and the toluene layer was replaced back into the round bottom flask. Following this step,  $\text{MnO}_2$  and  $\text{MgBr}$  were added to remove any residual water from the extraction and re-aromatize the product (Scheme 2). The product was dried using a rotary evaporator. Then, the product was purified using a silica column packed with hexane, and utilizing a solvent layer composed of 97% methylene chloride and 3% methanol.

*Synthesis of 5,6-dimethyl-2,9-disecbutyl-1,10-phenanthroline gold (III) complex (7)*

0.312 g of  $\text{NaAuCl}_4 \cdot 2\text{H}_2\text{O}$  was measured and added to 0.250 g of 5,6-dimethyl-2,9-disecbutyl-1,10-phenanthroline ligand in acetonitrile and refluxed for an hour, and then an acetonitrile solution containing 0.160 g of  $\text{AgBF}_4$  was added and the resulting reaction mixture refluxed overnight. The  $\text{AgCl}$  precipitate was filtered off and acetonitrile was removed by rotary evaporation (Scheme 3). The yellow solid synthesized was re-dissolved in a minimum amount of hot methanol. X-ray quality crystals were obtained by slowly evaporating the methanol.

*Synthesis of 4-methyl-2,9-disecbutyl-1,10-phenanthroline ligand (8)*

0.500 grams of the 4-dimethyl-2,9-disecbutyl-1,10-phenanthroline ligand was dissolved in anhydrous toluene under a nitrogen flow. An excess of sec-butyl lithium, 5 milliliters, was added drop-wise to the toluene reaction mixture. During this overnight reaction period, the round bottom flask was kept in ice water. After this overnight reaction, the reaction mixture was removed from the vessel, and the inorganic impurities and side products were removed using a liquid-liquid extraction. This extraction was performed twice with 50 milliliters of deionized water. The water layer was discarded and the toluene layer was replaced back into the round bottom flask. Following this step,  $\text{MnO}_2$  and  $\text{MgBr}$  were added to remove any residual water from the extraction and re-aromatize the product (Scheme 4). The product was dried using a rotary evaporator. Then, the product was purified using a silica gel slurry in hexane was used to pack the column, and utilizing a solvent layer composed of 97% methylene chloride and 3% methanol.

*Synthesis of 4-methyl-2,9-disecbutyl-1,10-phenanthroline gold (III) complex (9)*

0.328 g of  $\text{NaAuCl}_4 \cdot 2\text{H}_2\text{O}$  was measured and added to 0.250 g of 4-methyl-2,9-disecbutyl-1,10-phenanthroline ligand in acetonitrile and refluxed for an hour, and then an acetonitrile solution containing 0.165 g of  $\text{AgBF}_4$  was added and the resulting reaction mixture refluxed overnight. The  $\text{AgCl}$  precipitate was filtered off and acetonitrile was removed by rotary evaporation (Scheme 5). The yellow solid synthesized was re-dissolved in a minimum amount of hot methanol. X-ray quality crystals were obtained by slowly evaporating the methanol.

*Synthesis of 4,5,6,7-tetramethyl-2,9-disecbutyl-1,10-phenanthroline ligand (10)*

0.500 grams of the 4,5,6,7-tetramethyl-2,9-disecbutyl-1,10-phenanthroline ligand was dissolved in anhydrous toluene under a nitrogen flow. An excess of sec-butyl lithium, 5 milliliters, was added drop-wise to the toluene reaction mixture. During this overnight reaction period, the round bottom flask was kept in ice water. After this overnight reaction, the reaction mixture was removed from the vessel, and the inorganic impurities and side products were removed using a liquid-liquid extraction. This extraction was performed twice with 50 milliliters of deionized water. The water layer was discarded and the toluene layer was replaced back into the round bottom flask. Following this step,  $\text{MnO}_2$  and  $\text{MgBr}$  were added to remove any residual water from the extraction and re-aromatize the product (Scheme 6). The product was dried using a rotary evaporator. Then, the product was purified using a silica column packed with hexane, and utilizing a solvent layer composed of 97% methylene chloride and 3% methanol.

*Synthesis of 4,5,6,7-tetramethyl-2,9-disecbutyl-1,10-phenanthroline gold (III) complex (11)*

0.145 g of  $\text{NaAuCl}_4 \cdot 2\text{H}_2\text{O}$  was measured and added to 0.125 g of 4,5,6,7-tetramethyl-2,9-disecbutyl-1,10-phenanthroline ligand in acetonitrile and refluxed for an hour, and then an acetonitrile solution containing 0.085 g of  $\text{AgBF}_4$  was added and the resulting reaction mixture refluxed overnight. The  $\text{AgCl}$  precipitate was filtered off and acetonitrile was removed by rotary evaporation (Scheme 7). The yellow solid synthesized was re-dissolved in a minimum amount of hot methanol. X-ray quality crystals were obtained by slowly evaporating the methanol.

*Synthesis of 5-methyl-2,9-disecbutyl-1,10-phenanthroline ligand (12)*

0.500 grams of the 5-methyl-2,9-disecbutyl-1,10-phenanthroline ligand was dissolved in anhydrous toluene under a nitrogen flow. An excess of sec-butyl lithium, 5 milliliters, was added drop-wise to the toluene reaction mixture. During this overnight reaction period, the round bottom flask was kept in ice water. After this overnight reaction, the reaction mixture was removed from the vessel, and the inorganic impurities and side products were removed using a liquid-liquid extraction. This extraction was performed twice with 50 milliliters of deionized water. The water layer was discarded and the toluene layer was replaced back into the round bottom flask. Following this step,  $\text{MnO}_2$  and  $\text{MgBr}$  were added to remove any residual water from the extraction and re-aromatize the product (Scheme 8). The product was dried using a rotary evaporator. Then, the product was purified using a silica column packed with hexane, and utilizing a solvent layer composed of 97% methylene chloride and 3% methanol.

*Synthesis of 5-methyl-2,9-disecbutyl-1,10-phenanthroline gold (III) complex (13)*

0.163 g of  $\text{NaAuCl}_4 \cdot 2\text{H}_2\text{O}$  was measured and added to 0.125 g of 5-methyl-2,9-disecbutyl-1,10-phenanthroline ligand in acetonitrile and refluxed for an hour, and then an acetonitrile solution containing 0.091 g of  $\text{AgBF}_4$  was added and the resulting reaction mixture refluxed overnight. The  $\text{AgCl}$  precipitate was filtered off and acetonitrile was removed by rotary evaporation (Scheme 9). The yellow solid synthesized was re-dissolved in a minimum amount of hot methanol. X-ray quality crystals were obtained by slowly evaporating the methanol.

*X-ray crystallographic studies*

A suitable crystal of each ligand's gold complex was coated with Paratone N oil, suspended in a small fiber loop and placed in a cooled nitrogen gas stream at 173 K on a Bruker D8 APEX II CCD sealed tube diffractometer with graphite monochromated  $\text{Mo K}\alpha$  (0.71073 Å) radiation. Data were measured using a series of combinations of phi and omega scans with 10 s frame exposures and  $0.5^\circ$  frame widths. Data collection, indexing and initial cell refinements were all carried out using APEX II<sup>21</sup> software. Frame integration and final cell refinements were done using SAINT<sup>33</sup> software. The final cell parameters were determined from least-squares refinement on 1489 reflections. The structure was solved using direct methods and difference Fourier techniques (SHELXTL, V6.12)<sup>34</sup>. Hydrogen atoms were placed their expected chemical positions using the HFIX command and were included in the final cycles of least squares with isotropic  $U_{ij}$ 's related to the atoms ridden upon. All non-hydrogen atoms were refined anisotropically. Scattering factors and anomalous dispersion corrections are taken from the International Tables for X-ray Crystallography<sup>35</sup>. Structure solution, refinement, graphics and

generation of publication materials were performed by using SHELXTL, v6.12 software.

### *Buffer Stability studies*

For the stability studies with the phenanthroline ligands, a  $5 \times 10^{-3}$  M stock solution of each of the gold complexes was prepared in 4.00 mL acetonitrile.  $5 \times 10^{-3}$  M stock solutions were also prepared for ascorbic acid and glutathione in phosphate buffer. To complete the buffer stability study, 7  $\mu$ L of the gold complex stock solution was taken and diluted to a volume of 4 mL using a 0.1 M phosphate buffer. The glutathione (GSH) stability study was conducted by adding 7  $\mu$ L of the gold complex stock solution to 12  $\mu$ L of the GSH stock solution. This was then also diluted to a volume of 4 mL using a 0.1 M phosphate buffer. The ascorbic acid study was conducted by adding 7  $\mu$ L of the gold complex stock solution to 8  $\mu$ L of the ascorbic acid stock solution, which was then diluted to a volume of 4 mL using a 0.1 M phosphate buffer. Complexes were analyzed by UV-vis sampling over a period for 24 hours at thirty-seven degrees Celsius to collect this data.

### *GSH Buffer stability studies – Dipyridyl Ligands*

Compound **4** was dissolved in a minimum amount of DMSO, and then diluted in 10 mM phosphate buffer (pH 7.4, 20 mM NaCl,  $5 \times 10^{-5}$  M reduced glutathione) to a final concentration of  $5 \times 10^{-5}$  M. This solution was analyzed by UV-vis spectroscopy at 37°C once every hour for 24 hours.

### *DNA binding studies- Dipyridyl Ligands*

A solution containing compound **4** ( $5 \times 10^{-5}$  M) and calf thymus DNA was made by combining 4.76 mL of 1 mg/mL DNA solution, the appropriate amount of a 5 mg/mL stock solution of compound **4** in DMSO, and enough phosphate buffer (pH 7.4, 20 mM NaCl) to make 5 mL total volume. The solution was incubated at 37°C for 24 hours in a shaker at 150

rev/min. The solution was filtered through a 10,000 MW spin filter and the flow-through analyzed by UV-Vis spectroscopy. A control solution of  $5 \times 10^{-5}$  M gold compound in buffer possessing no DNA was treated in a similar manner.

*DNA Binding Studies- Phenanthroline Ligands*

A  $1.5 \times 10^{-3}$  M stock solution was prepared by dissolving 0.010g of calf thymus DNA in 10mL of 10mM phosphate buffer. A gold complex concentration of  $1 \times 10^{-5}$  M was utilized for this study, with 10 base pairs of DNA for each molecule of the gold (III) complex. After an hour of incubation at 37°C, the solution was filtered through a 10,000 MW spin filter and the flow-through analyzed by UV-Vis spectroscopy.

## Results and Discussion

### *Synthesis*

The dipyriddy sulfide ligand was prepared as previously reported in the 1980 Perkins' paper (final pure oil was isolated via Kugelrohr distillations: 0.1 torr/150°C).<sup>36</sup> Dipyriddy oxide, the ligand for the compound **2**, was synthesized with equal amounts of 2-hydroxypyridine and bromopyridine. The dipyriddy ketone was purchased. Each of the ligands were then reacted with NaAuCl<sub>4</sub> in a round bottom flask. After refluxing for approximately an hour, AgBF<sub>4</sub> was added. Following the addition of the AgBF<sub>4</sub>, the reaction was allowed to reflux overnight. The gold complex was filtered through a funnel with Celite, and the filtrate was recrystallized to form the finalized crystalline gold complex (Yields- see Table 1).

The *sec*-butyl-phenanthroline ligands were prepared as denoted in the experimental section above. Following purification by column chromatography, the yields of the 5,6-dimethyl-2,9-disecbutyl-1,10-phenanthroline ligand and the 4-methyl-2,9-disecbutyl-1,10-phenanthroline ligand were high enough to proceed to the gold reaction directly. The yields of 4,5,6,7-tetramethyl-2,9-disecbutyl-1,10-phenanthroline ligand and the 5-methyl-2,9-disecbutyl-1,10-phenanthroline ligand were minimal, thus requiring multiple rounds of ligand synthesis before enough was acquired to conduct the gold reactions. (Yields – See Table 2)

Compound #	<b>1</b>	<b>2</b>	<b>3</b>	<b>4</b>	<b>5</b>
Yield (average)	.247	.092	.123	.106	.084

Table 2. Yields for the Dipyriddy Ligands and Respective Gold Complexes



Compound #	6	7	8	9	10	11	12	13
Yield (average)	.257	.132	.128	.106	.042	.118	.035	.173

Table 3. Yields for the Phenanthroline Ligands and Respective Gold Complexes

### *<sup>1</sup>H NMR and UV-vis Spectroscopy*

The peaks and chemical shifts of the dipyriddy oxide in deuterated chloroform utilizing the Mercury 300, are 8.22 (doublet of doublets, 2H), 7.69 (triplet of doublets, 2H), 7.04 (doublet of doublets, 2H), 7.00 (doublet of doublets, 2H). The complexing of the dipyriddy oxide ligand with gold created an asymmetry in the aromatic protons and shifted the aromatic peaks downfield. The peaks and chemical shifts for the gold complex are 8.46 (doublet, 1H), 8.28 (doublet, 1H), 8.09 (triplet, 1H), 7.91 (triplet, 1H), 7.67 (doublet, 1H), 7.46 (triplet, 1H), 7.34 (doublet, 1H), 7.28 (triplet, 1H).

NMR spectroscopy in deuterated chloroform, utilizing the Mercury 300, was also used to study the 4-methyl-2,9-disecbutyl-1,10-phenanthroline ligand, the 5,6-dimethyl-2,9-disecbutyl-1,10-phenanthroline ligand, the 5,6-dimethyl-2,9-disecbutyl-1,10-phenanthroline gold(III) complex, and the 4-methyl-2,9-disecbutyl-1,10-phenanthroline gold(III) complex. The spectrum for compound **6** demonstrated relative purity following flash column chromatography with a solvent of methylene chloride and methanol. Compound **8** was also purified by column chromatography. As Figure 1 illustrates, the ligand has the following peaks and shifts: 8.15 (doublet, 1H), 7.90 (doublet, 1H), 7.70 (doublet, 1H), 7.50 (doublet, 2H), 3.27 (multiplet, 2H), and 2.75 (singlet, 3H). The NMR spectra of the gold complexes exhibited the expected peaks

and shifts from the ligands' spectra. For compound **7**, as shown in Figure 2, the peaks and shifts present on the spectrum are 8.66 (doublet, 2H), 7.83 (doublet, 2H), 4.54 (multiplet, 2H), 2.78 (singlet, 5H), 1.56 (doublet, 3H), and 1.03 (triplet, 3H). The spectrum for compound **9**, shown in Figure 3, has the following peaks and chemical shifts: 8.41 (doublet, 1H), 8.08 (doublet, 1H), 7.99 (doublet, 1H), 7.82 (doublet, 1H), 7.64 (singlet, 1H), 4.64 (multiplet, 1H), 4.34 (multiplet, 1H), 2.06 (multiplet, 2H), 1.85 (multiplet, 2H), 1.55 (multiplet, 9H), and 1.04 (multiplet, 5H). The spectra have some shifts not expected from a pure form of the ligand or gold complexes, indicating either the solvent or possible impurities.

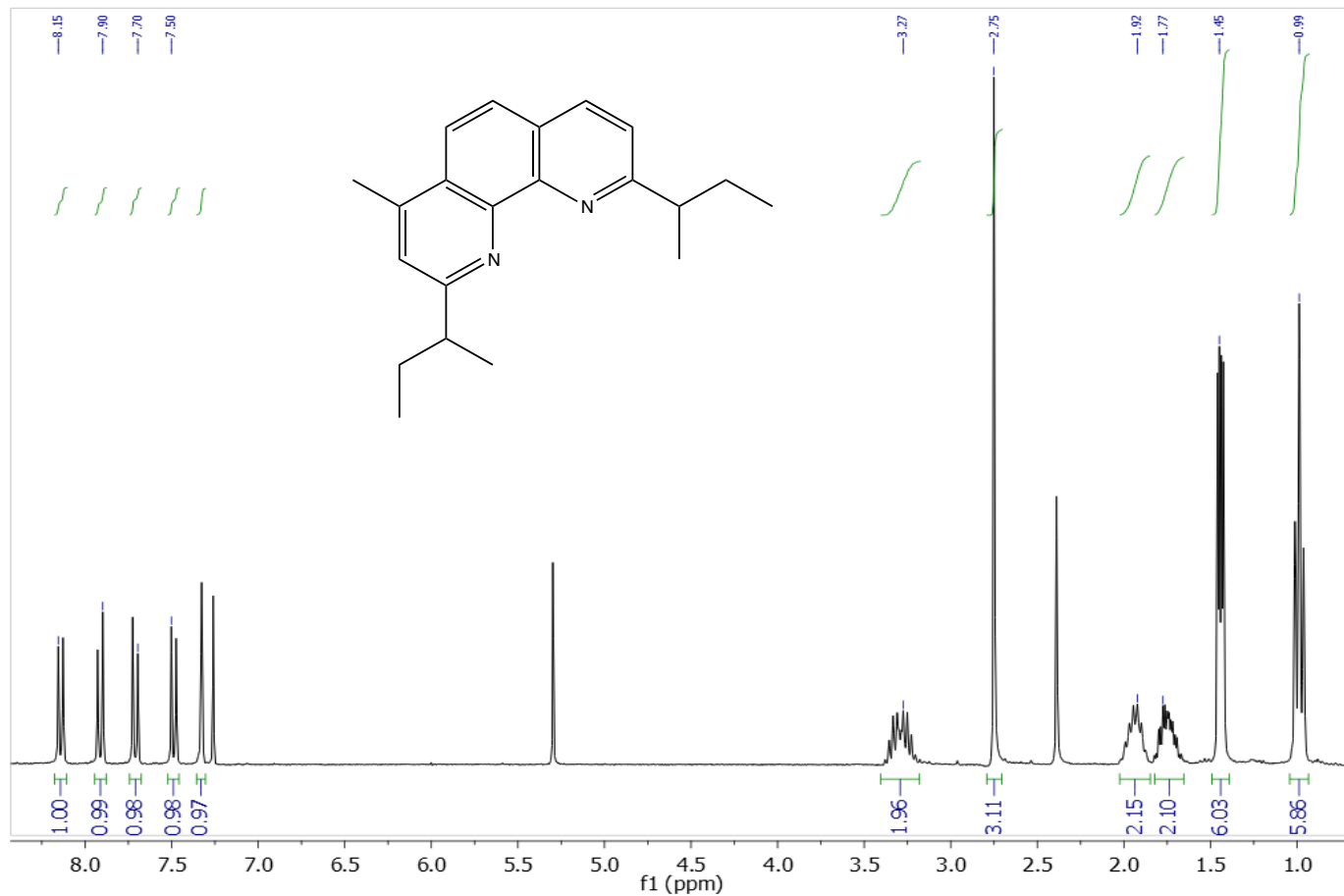


Figure 1. NMR Spectroscopy of 4-methyl-2,9-diisobutyl-1,10-phenanthroline ligand (recorded in CDCl<sub>3</sub>). The five aromatic protons are present in the expected range (around 7-8.25ppm) while the sec-butyl protons and methyl protons present around the hydrocarbon region (1-3.5ppm). The integrals support the number of protons predicted by the expected ligand product. Methylene chloride accounts for the peak around 5.35ppm.

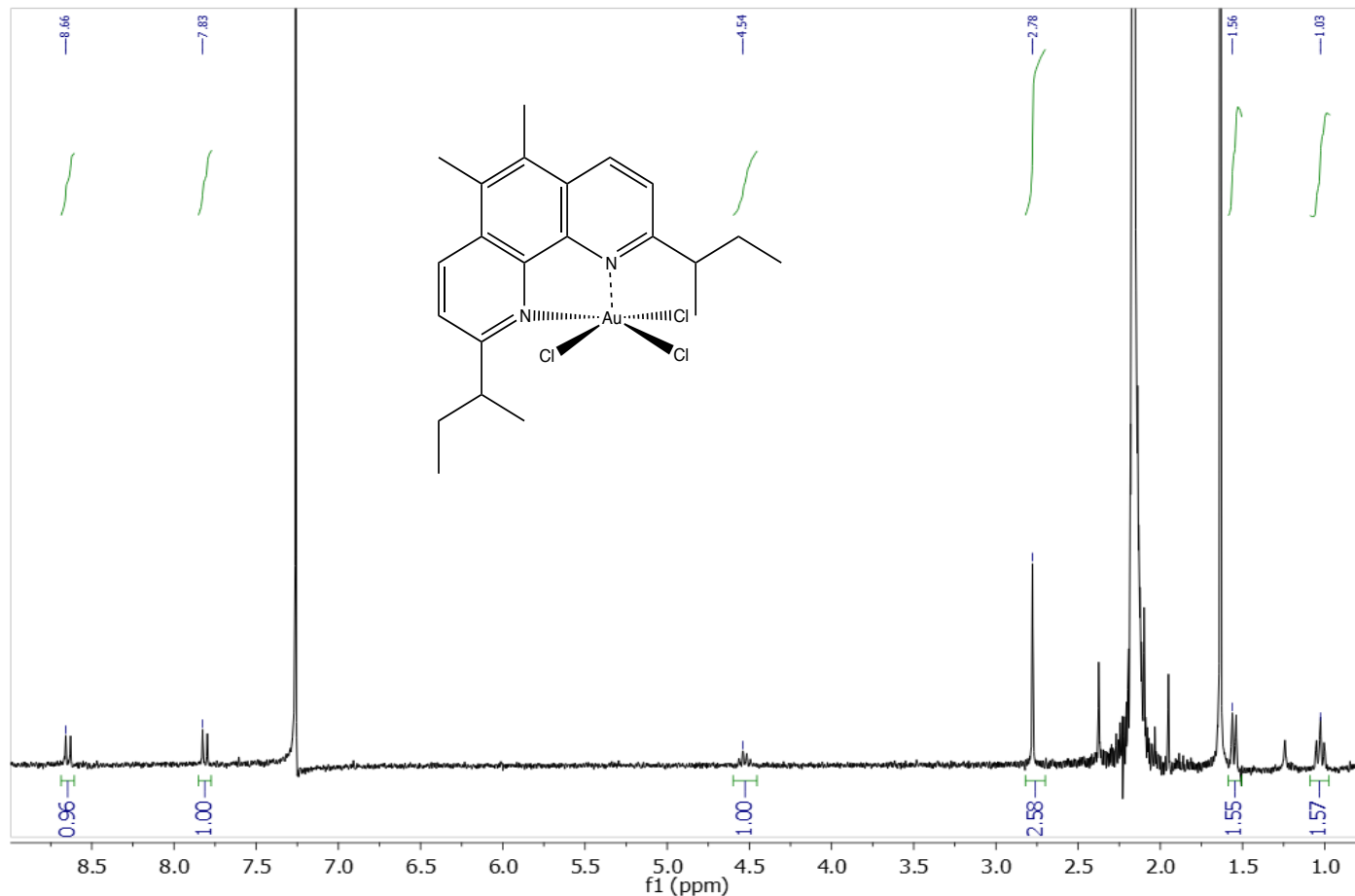


Figure 2. NMR Spectroscopy of 5,6-dimethyl-2,9-disebutyl-1,10-phenanthroline gold(III) complex (recorded in  $\text{CDCl}_3$ ). Because of the symmetry present on the backbone, there are only two different natured protons, supported by the two different aromatic peaks in the aromatic region. The expected sec-butyl, and methyl protons are present in the hydrocarbon region. The peak around 7.25 is a solvent peak present, not representative of the gold complex.

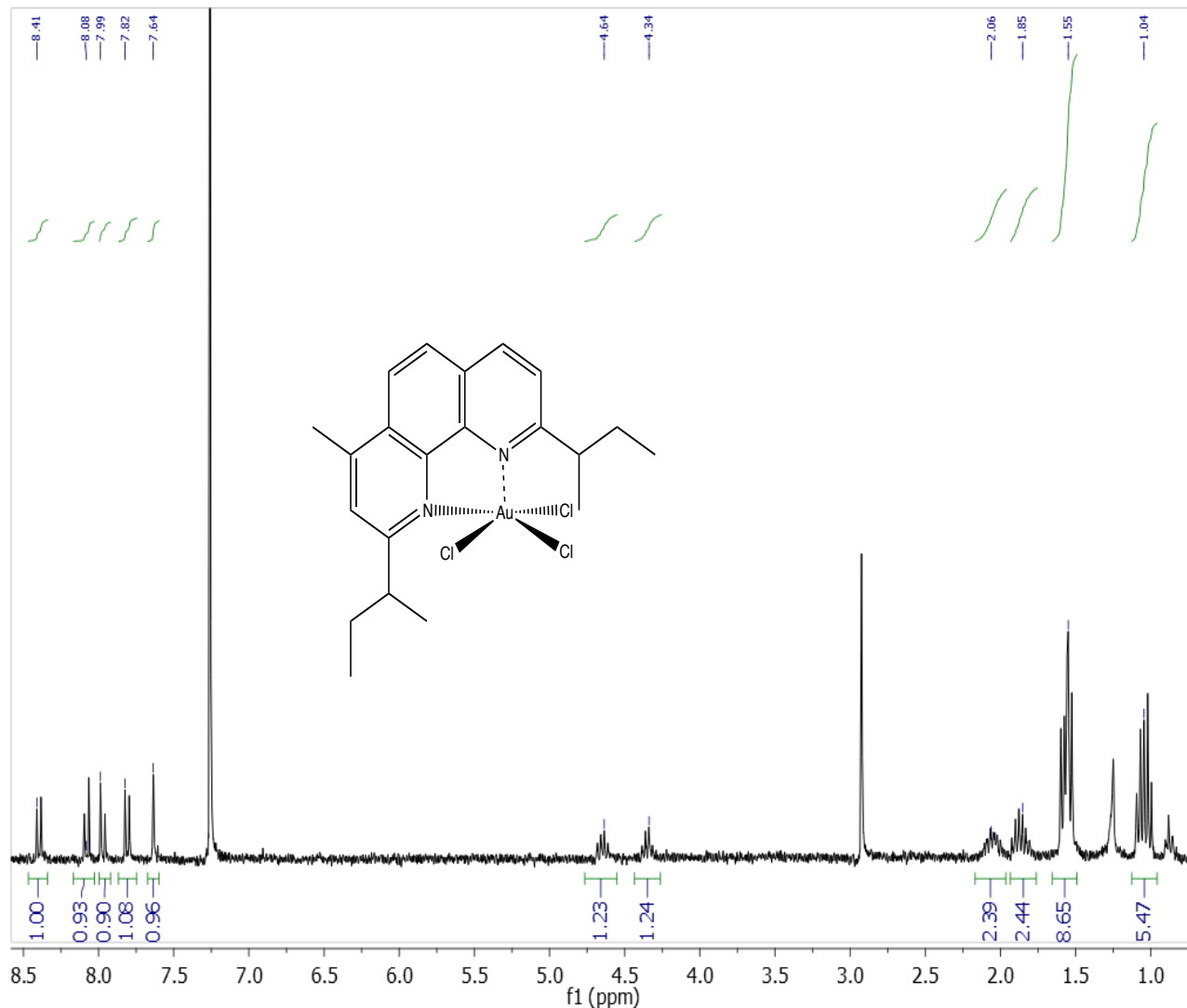


Figure 3. NMR Spectroscopy of 4-methyl-2,9-disebutyl-1,10-phenanthroline gold(III) complex (recorded in  $\text{CDCl}_3$ ). The five aromatic protons are present, and because of the complexation with gold, the protons are shifted from the expected range (around 7-8.25ppm) to 7.5-8.5 ppm. Since the sec-butyl protons were in close proximity to the gold, they experienced a shift from around 2-3.5ppm to 4.3-4.75ppm. The methyl protons present a small shift, from 1-1.6ppm to 1.15-1.85ppm. The integrals support the number of protons predicted by the expected ligand product.

### *X-Ray Crystal Structures*

The X-ray crystal structure of the dipyriddy oxide gold (III) depicted a unimolecular complex (Figure 4). The complex is asymmetric and monodentate with a square planar molecular geometry. The proposed identification of the molecular geometry as square planar is supported by the following bond angles: N(1)-Au(1)-Cl(3), Cl(1)-Au(1)-Cl(3), N(1)-Au(1)-Cl(2), and Cl(1)-Au(1)-Cl(2). These angles ranged from 88.76 – 90.95°. This monodentate X-ray crystal structure was supported by a previous report, with a square planar geometry and similar bond lengths.<sup>37</sup> The X-ray crystal structure of dipyriddy ketone gold(III) illustrated the ligand was unsuccessful in complexing with the gold tetrachlorate (Figure 5). One hypothesis for this failed complexing was because of the  $sp^2$  hybridization, generating a much wider bite angle in the ligand. The X-ray crystal structure of the dipyriddy sulfide gold (III) depicted two molecules composing the complex ion, the dipyriddy sulfide  $AuCl_2^{+1}$  and  $AuCl_4^{-1}$  (Figure 6). The complex demonstrated bidentate binding and was symmetric. The molecular geometry of the complex is square planar, which is supported by the following bond angles: N(1)-Au(1)-N(1)A, N(1)-Au(1)-Cl(1), N(1)A-Au(1)-Cl(1)A, Cl(1)-Au(1)-Cl(1)A, N(2)A-Au(2)-N(2), N(2)A-Au(2)-Cl(2)A, N(2)-Au(2)-Cl(2), Cl(2)A-Au(2)-Cl(2), Cl(8)-Au(3)-Cl(7), Cl(6)-Au(3)-Cl(7), Cl(8)-Au(3)-Cl(9), Cl(6)-Au(3)-Cl(9), Cl(5)-Au(4)-Cl(3)A, Cl(4)-Au(4)-Cl(3)A, Cl(5)-Au(4)-Cl(3), and Cl(4)-Au(4)-Cl(3). A previous reported bidentate gold complex in Dalton supported the experimental data from this experiment, with similar bond lengths and a square planar geometry.<sup>38</sup>

An X-ray crystal structure was also generated for the 5,6-dimethyl-2,9-disecbutyl-1,10-phenanthroline gold(III) complex (Figure 7). The complex is symmetric and bidentate with a distorted square pyramidal geometry. The proposed identification of the molecular geometry as distorted square pyramidal is supported by the following bond angles: N(2)-Au(1)-Cl(1), N(2)-Au(1)-Cl(2), Cl(1)-Au(1)-Cl(3), Cl(2)-Au(1)-Cl(3), Cl(1)-Au(1)-N(1), and Cl(2)-Au(1)-N(1). These angles ranged from 86.0 – 93.0°. The bond lengths for Au(1)-N(1) of 2.579 angstroms, and Au(1)-N(2) of 2.085 angstroms also support this square pyramidal geometry. The distortion is apparent in two of the bond angles: Cl(3)-Au(1)-N(1) of 112.8° and N(2)-Au(1)-N(1) of 71.3°, which were expected to be 90°. This bidentate X-ray crystal structure was supported by a previous report, with a square pyramidal geometry.<sup>38</sup>

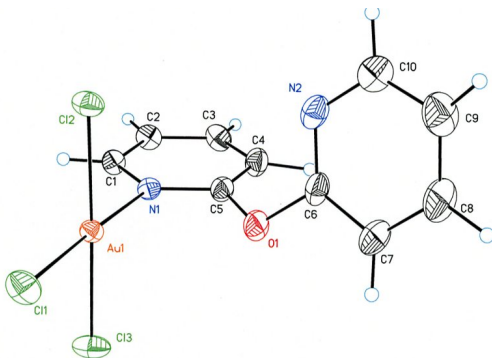


Figure 4: X-ray crystal structure of Dipyriddy oxide AuCl<sub>3</sub>. Selected bond distances (Å) and angles (°): Au(1)-N(1), 2.040(2); Au(1)-Cl(1), 2.2576(7); Au(1)-Cl(3), 2.2692(7); Au(1)-Cl(2), 2.2850(6); N(1)-Au(1)-Cl(1), 176.99(6); N(1)-Au(1)-Cl(3), 90.00(5); Cl(1)-Au(1)-Cl(3), 90.41(2); N(1)-Au(1)-Cl(2), 88.76(5); Cl(1)-Au(1)-Cl(2), 90.95(2); Cl(3)-Au(1)-Cl(2), 177.29(2); C(5)-N(1)-Au(1), 118.16(17); C(1)-N(1)-Au(1), 121.46(17).

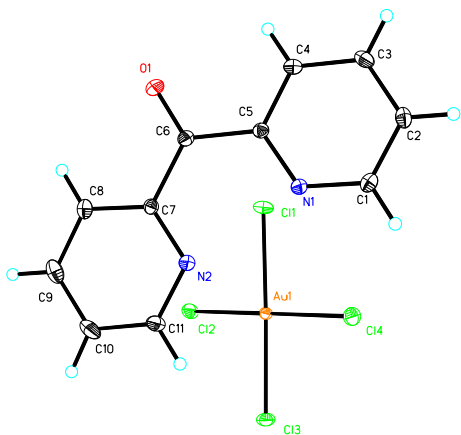


Figure 5: Dipyriddy Ketone with Gold(III). Selected bond distances (Å) and angles (°): Au(1)-Cl(3), 2.2768(8); Au(1)-Cl(2), 2.2812(7); Au(1)-Cl(1), 2.2878(8); Au(1)-Cl(4), 2.2887(7); Cl(3)-Au(1)-Cl(2), 90.35(3); Cl(3)-Au(1)-Cl(1), 178.18(3); Cl(2)-Au(1)-Cl(1), 89.40(3); Cl(3)-Au(1)-Cl(4), 89.35(3); Cl(2)-Au(1)-Cl(4), 178.55(3); Cl(1)-Au(1)-Cl(4), 90.94(3).



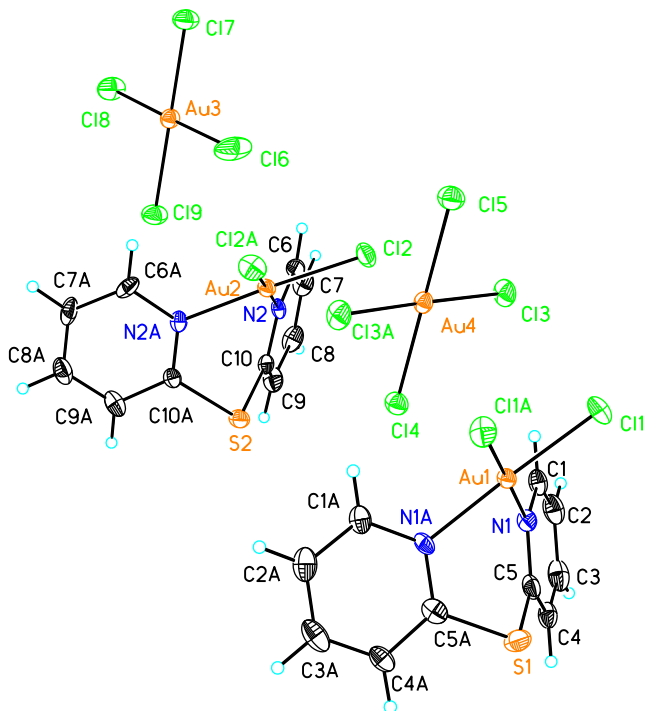
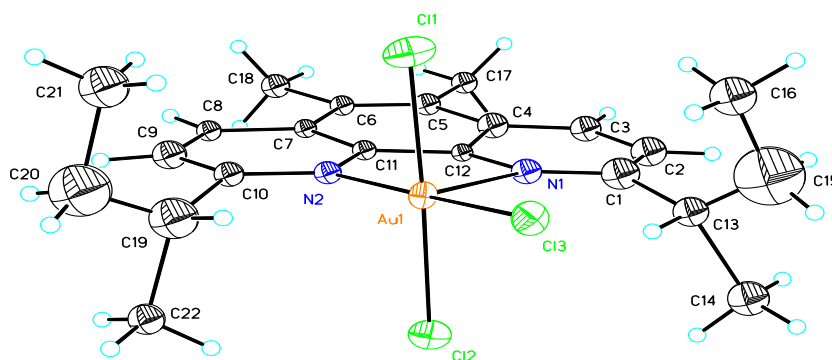


Figure 6. Dipyridyl Sulfide with Gold(III). Selected bond distances ( $\text{\AA}$ ) and angles ( $^\circ$ ): Au(1)-N(1), 2.037(5); Au(1)-N(1)A, 2.037(5); Au(1)-Cl(1), 2.2453(16); Au(1)-Cl(1)A, 2.2453(16); Au(2)-N(2)A, 2.028(5); Au(2)-N(2), 2.028(5); Au(2)-Cl(2)A, 2.2436(16); Au(2)-Cl(2), 2.2436(16); Au(3)-Cl(8), 2.253(3); Au(3)-Cl(6), 2.263(3); Au(3)-Cl(7), 2.272(2); Au(3)-Cl(9), 2.277(2); Au(4)-Cl(5), 2.273(2); Au(4)-Cl(4), 2.281(2); Au(4)-Cl(3)A, 2.2829(16); Au(4)-Cl(3), 2.2829(16); N(1)-Au(1)-N(1)A, 89.1(3); N(1)-Au(1)-Cl(1), 89.90(15); N(1)#1-Au(1)-Cl(1), 177.90(16); N(1)-Au(1)-Cl(1)A, 177.90(16); N(1)A-Au(1)-Cl(1)A, 89.90(15); Cl(1)-Au(1)-Cl(1)A, 91.09(9); N(2)A-Au(2)-N(2), 88.1(3); N(2)A-Au(2)-Cl(2)A, 91.16(14); N(2)-Au(2)-Cl(2)A, 177.49(15); N(2)A-Au(2)-Cl(2), 177.48(15); N(2)-Au(2)-Cl(2), 91.16(14); Cl(2)A-Au(2)-Cl(2), 89.44(9); Cl(8)-Au(3)-Cl(6), 178.99(10); Cl(8)-Au(3)-Cl(7), 90.44(9); Cl(6)-Au(3)-Cl(7), 88.55(10); Cl(8)-Au(3)-Cl(9), 89.39(9); Cl(6)-Au(3)-Cl(9), 91.62(10); Cl(7)-Au(3)-Cl(9), 179.83(10); Cl(5)-Au(4)-Cl(4), 179.95(9); Cl(5)-Au(4)-Cl(3)A, 90.19(4); Cl(4)-Au(4)-Cl(3)A, 89.81(4); Cl(5)-Au(4)-Cl(3), 90.19(4); Cl(4)-Au(4)-Cl(3), 89.81(4); Cl(3)A-Au(4)-Cl(3), 178.12(9).



**Figure 7:** X-ray Crystal Structure. Selected bond lengths (Å) and angles (°): Au(1)-N(2) 2.085(11), Au(1)-Cl(1) 2.263(4), Au(1)-Cl(2) 2.274(4), Au(1)-Cl(3) 2.279(3), Au(1)-N(1) 2.579(11), N(2)-Au(1)-Cl(1) 86.0(3), N(2)-Au(1)-Cl(2) 92.0(3), Cl(1)-Au(1)-Cl(2) 177.67(15), N(2)-Au(1)-Cl(3) 175.3(3), Cl(1)-Au(1)-Cl(3) 91.35(13), Cl(2)-Au(1)-Cl(3) 90.59(13), N(2)-Au(1)-N(1) 71.3(4), Cl(1)-Au(1)-N(1) 93.0(3), Cl(2)-Au(1)-N(1) 87.5(3), Cl(3)-Au(1)-N(1) 112.8(3) .

**Table 4.** Crystal data and structure refinement for Dipyriddyloxide AuCl<sub>3</sub>

Identification code	JFEXV_33	
Empirical formula	C <sub>10</sub> H <sub>8</sub> Au Cl <sub>3</sub> N <sub>2</sub> O	
Formula weight	475.50	
Temperature	172(2) K	
Wavelength	0.71073 Å	
Crystal system	Monoclinic	
Space group	C2/c	
Unit cell dimensions	a = 24.746(2) Å	a = 90°.
	b = 7.6040(7) Å	b = 112.7450(10)°.
	c = 15.3576(14) Å	g = 90°.
Volume	2665.1(4) Å <sup>3</sup>	
Z	8	
Density (calculated)	2.370 Mg/m <sup>3</sup>	
Absorption coefficient	11.625 mm <sup>-1</sup>	
F(000)	1760	
Crystal size	0.23 x 0.12 x 0.10 mm <sup>3</sup>	
Theta range for data collection	1.78 to 30.23°.	
Index ranges	-33 ≤ h ≤ 34, -10 ≤ k ≤ 10, -21 ≤ l ≤ 21	
Reflections collected	23715	
Independent reflections	3765 [R(int) = 0.0344]	
Completeness to theta = 30.23°	94.7 %	
Absorption correction	Semi-empirical from equivalents	
Max. and min. transmission	0.3894 and 0.1751	

Refinement method	Full-matrix least-squares on $F^2$
Data / restraints / parameters	3765 / 0 / 186
Goodness-of-fit on $F^2$	1.024
Final R indices [ $I > 2\sigma(I)$ ]	$R_1 = 0.0170$ , $wR_2 = 0.0442$
R indices (all data)	$R_1 = 0.0193$ , $wR_2 = 0.0451$
Largest diff. peak and hole	1.301 and -1.192 e. $\text{\AA}^{-3}$

**Table 5.** Crystal data and structure refinement for Dipyrindyl Ketone with Gold(III).

Identification code	jflexv20s	
Empirical formula	C <sub>11</sub> H <sub>8</sub> Au Cl <sub>4</sub> N <sub>2</sub> O	
Formula weight	522.96	
Temperature	293(2) K	
Wavelength	0.71073 $\approx$	
Crystal system	Monoclinic	
Space group	P2(1)/c	
Unit cell dimensions	$a = 8.0231(10) \approx$	$a = 90^\circ$ .
	$b = 24.158(3) \approx$	$b = 93.111(2)^\circ$ .
	$c = 7.3908(9) \approx$	$g = 90^\circ$ .
Volume	1430.4(3) $\approx^3$	
Z	4	
Density (calculated)	2.428 Mg/m <sup>3</sup>	
Absorption coefficient	11.022 mm <sup>-1</sup>	
F(000)	972	
Crystal size	0.36 x 0.16 x 0.14 mm <sup>3</sup>	
Theta range for data collection	1.69 to 30.21 $^\circ$ .	
Index ranges	-11 $\leq h \leq$ 11, -33 $\leq k \leq$ 33, -10 $\leq l \leq$ 10	
Reflections collected	26112	
Independent reflections	4036 [ $R(\text{int}) = 0.0352$ ]	
Completeness to $\theta = 30.21^\circ$	94.9 %	
Absorption correction	Semi-empirical from equivalents	
Refinement method	Full-matrix least-squares on $F^2$	
Data / restraints / parameters	4036 / 0 / 172	
Goodness-of-fit on $F^2$	1.112	
Final R indices [ $I > 2\sigma(I)$ ]	$R_1 = 0.0199$ , $wR_2 = 0.0462$	
R indices (all data)	$R_1 = 0.0221$ , $wR_2 = 0.0469$	
Largest diff. peak and hole	1.272 and -1.609 e. $\approx^{-3}$	

**Table 6.** Crystal data and structure refinement for Dipyriddy Sulphide with Gold(III)

Identification code	jfe_xv_ii	
Empirical formula	C <sub>10</sub> H <sub>8</sub> Au <sub>2</sub> Cl <sub>6</sub> N <sub>2</sub> S	
Formula weight	794.88	
Temperature	172(2) K	
Wavelength	0.71073 Å	
Crystal system	Orthorhombic	
Space group	Pnma	
Unit cell dimensions	a = 16.047(4) Å	a = 90°.
	b = 12.081(3) Å	b = 90°.
	c = 17.889(5) Å	g = 90°.
Volume	3468.1(15) Å <sup>3</sup>	
Z	8	
Density (calculated)	3.045 Mg/m <sup>3</sup>	
Absorption coefficient	17.937 mm <sup>-1</sup>	
F(000)	2864	
Crystal size	0.13 x 0.06 x 0.03 mm <sup>3</sup>	
Theta range for data collection	1.70 to 30.50°.	
Index ranges	-21 ≤ h ≤ 22, -17 ≤ k ≤ 16, -25 ≤ l ≤ 23	
Reflections collected	56980	
Independent reflections	5327 [R(int) = 0.1032]	
Completeness to theta = 30.50°	96.6 %	
Absorption correction	Semi-empirical from equivalents	
Max. and min. transmission	0.6152 and 0.2039	
Refinement method	Full-matrix least-squares on F <sup>2</sup>	
Data / restraints / parameters	5327 / 0 / 208	
Goodness-of-fit on F <sup>2</sup>	1.040	
Final R indices [I > 2σ(I)]	R1 = 0.0361, wR2 = 0.0647	
R indices (all data)	R1 = 0.0687, wR2 = 0.0730	
Largest diff. peak and hole	2.574 and -1.608 e.Å <sup>-3</sup>	

### *Buffer Stability*

The dipyriddy oxide gold(III) exhibited poor stability in slightly basic buffer. The stability of the dipyriddy oxide complex was tested over a period of 24 hours by collecting UV-vis absorption data hourly. After the first hour, the gold absorption severely dropped; following this initial drop in absorption, the gold peak remained fairly stable.

In contrast, the 5,6-dimethyl-2,9-disecbutyl-1,10-phenanthroline gold(III) complex and the 4-methyl-2,9-disecbutyl-1,10-phenanthroline gold(III) complex demonstrated stability in slightly basic buffer, with minimal degradation of the gold peak over the period of 24 hours (Figure 8 and Figure 9 respectively). This is more apparent in the spectrum of compound **7** because both the ligand and the gold peaks remained fairly constant, with an overlay of the hourly studies. The spectrum of the compound **9** demonstrates a slight increase in the gold peak from the second and third hours to the finish of the study at 24 hours. A possible explanation for this is an evaporation of solvent from the cuvette. The absence of the gold(I) peak also supports this explanation. Another possible explanation of this change in absorbance is the binding constant of the complex; as the cuvette is heated, the amount of the complex that dissolves in the buffer increases with the added heat from the UV-vis instrument. Thus, compound **7** and compound **9** both demonstrated stability with little to no degradation of the ligand-metal charge transfer peak over the time period of the study, with the dimethyl phenanthroline gold complex being even more stable than the asymmetric ligand.

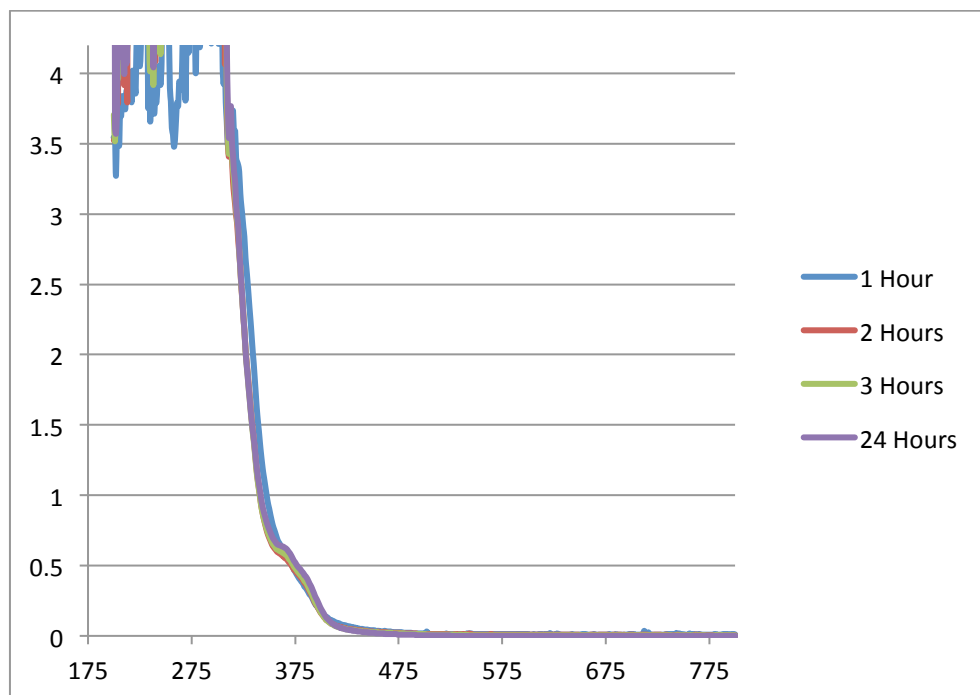


**Figure 8:** Buffer stability of 5,6-dimethyl-2,9-disecbutyl-1,10-phenanthroline gold(III) complex ( $5 \times 10^{-5}$  M) in 10 mM phosphate (pH 7.4, 20 mM NaCl) at  $37^{\circ}\text{C}$ . Spectra collected once every hour for 24 hours.

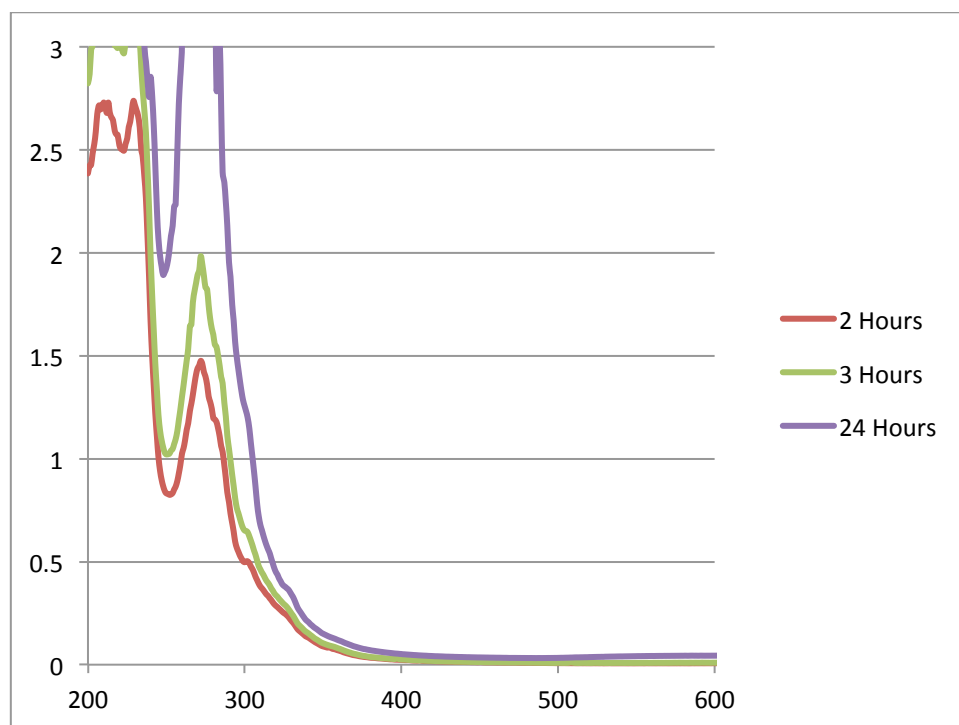


**Figure 9:** Buffer stability of 4-methyl-2,9-disecbutyl-1,10-phenanthroline gold(III) complex ( $5 \times 10^{-5}$  M) in 10 mM phosphate (pH 7.4, 20 mM NaCl) at  $37^{\circ}\text{C}$ . Spectra collected once every hour for 24 hours.

### *GSH Buffer Stability*

The stability of compound **2** was also tested in the presence of the biological reductant, glutathione (GSH) (Figure 10). The GSH stability test was conducted by collecting UV-vis absorption data over a period of 24 hours for a stock of complex **2** with buffer and GSH. Over the period of 24 hours, the dipyriddy oxide gold complex appeared to have fairly poor stability, as evident by the notable degradation of the ligand-metal charge transfer peak within the first hour, although the peak remained stable following this first hour.

GSH stability studies were also conducted for the 5,6-dimethyl-2,9-disecbutyl-1,10-phenanthroline gold(III) complex and the 4-methyl-2,9-disecbutyl-1,10-phenanthroline gold(III) complex (Figure 11 and Figure 12 respectively). Both of these complexes demonstrated stability in the presence of GSH. Compound **7** exhibits steady stability over the 24 hours study period with no degradation or shifting of any peaks. The spectrum for compound **9** demonstrated an increase in absorbance over the 24 hours, with no degradation of the gold peak. Evaporation is a possible cause for part of this increase. Another possible explanation of this change in absorbance is that we are observing a change in the binding constant of the ligand to the gold complex as the cuvette is heated.

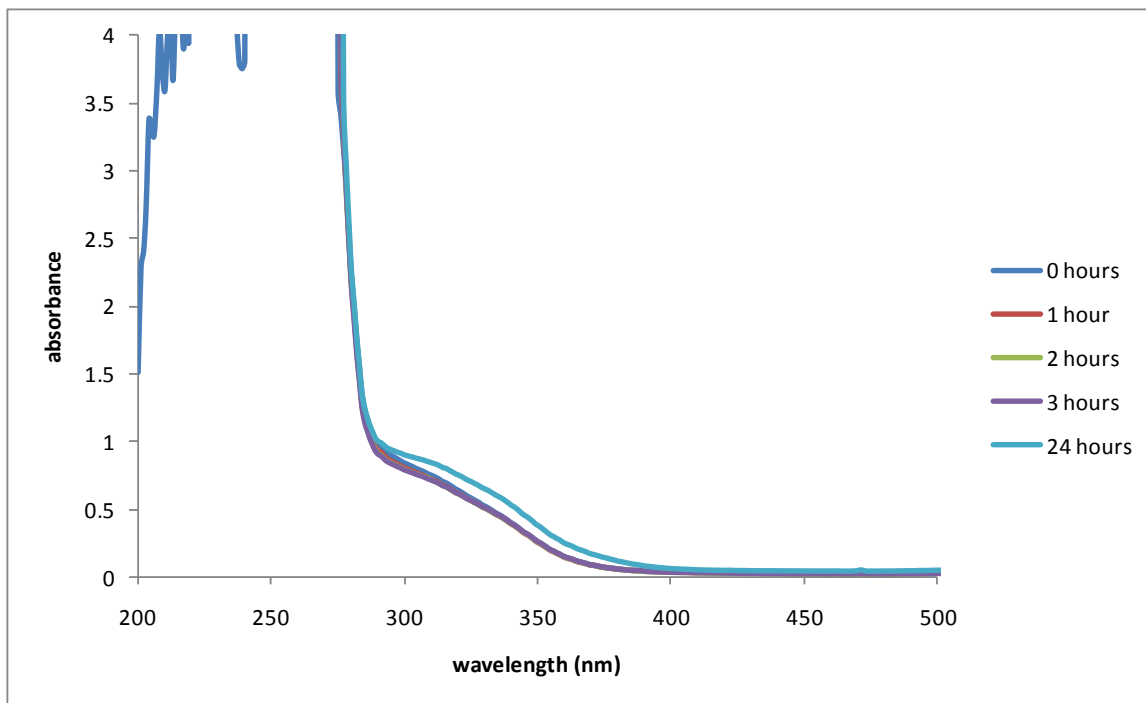


**Figure 10:** GSH stability of compound **2** ( $5 \times 10^{-5}$  M) in 10 mM phosphate (pH 7.4, 20 mM NaCl,  $5 \times 10^{-5}$  M GSH) at 37°C. Spectra collected once every hour for 24 hours.

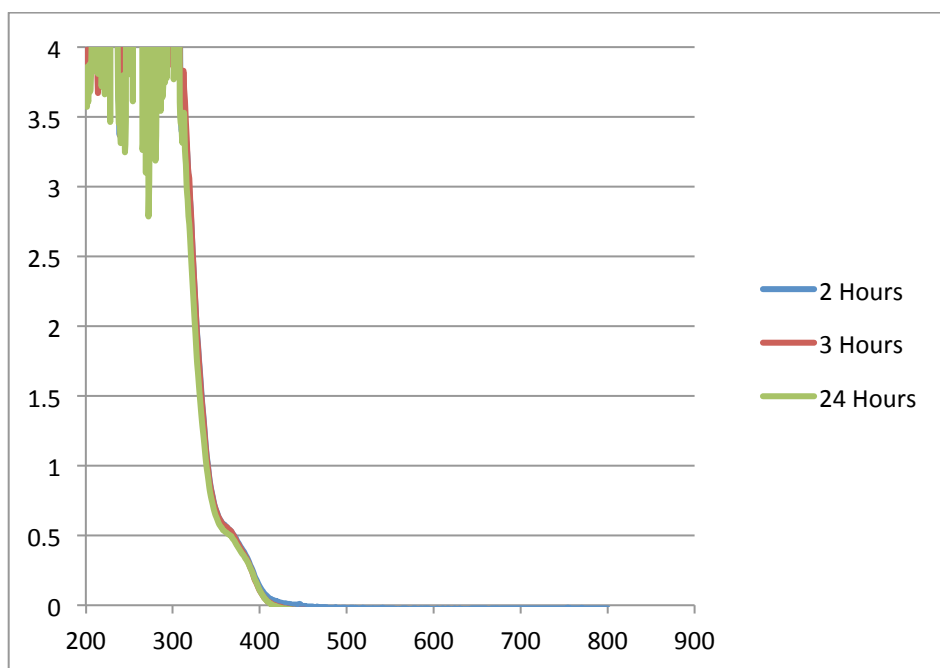


**Figure 11:** GSH stability of 5,6-dimethyl-2,9-disecbutyl-1,10-phenanthroline gold(III) complex ( $5 \times 10^{-5}$  M) in 10 mM phosphate (pH 7.4, 20 mM NaCl,  $5 \times 10^{-5}$  M GSH) at 37°C. Spectra collected once every hour for 24 hours.



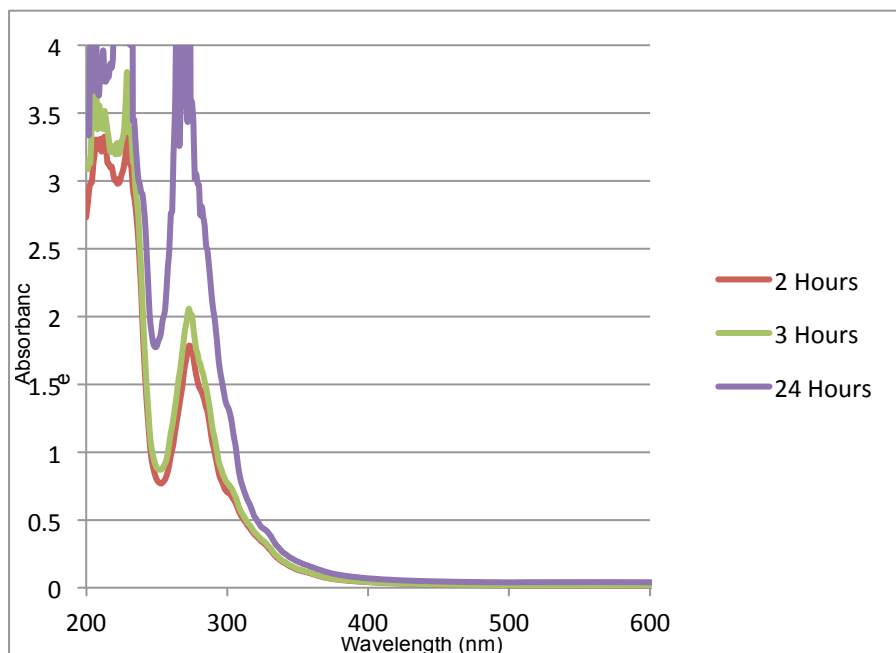


**Figure 12:** GSH stability of 4-methyl-2,9-disecbutyl-1,10-phenanthroline gold(III) complex ( $5 \times 10^{-5}$  M) in 10 mM phosphate (pH 7.4, 20 mM NaCl,  $5 \times 10^{-5}$  M GSH) at 37°C. Spectra collected once every hour for 24 hours.

#### *Ascorbic Acid Stability*

Ascorbic acid stability studies were conducted for the phenanthroline gold (III) complexes. The resulting spectra from these studies demonstrated some instability in the presence of this stronger biological reductant. The spectrum from the 5,6-dimethyl-2,9-disecbutyl-1,10-phenanthroline gold(III) complex is ambiguous in that the gold shoulder increases over the 24 hours study (Figure 13). None of the peaks are shifted and no clear gold (I) peak is present. However, because of the increase in the gold shoulder, no conclusive derivations can be pulled from this spectrum.

The spectrum for the 4-methyl-2,9-disecbutyl-1,10-phenanthroline gold(III) complex demonstrated an initial drop in the gold (III) peak (Figure 14). This decrease in the gold (III) absorbance peak continued steadily throughout the study, as demonstrated by the decreasing of

the peak centered around 350 nm; concomitant with that decrease, there is an increase in the peak centered around 330 nm, consistent with free ligand. Although both of the stability studies appeared to present flawed results, there seems to be enough evidence to indicate that the complexes can demonstrate a slight instability in these in vitro ascorbic acid buffer environments. The results of the studies suggested that the two gold complexes were both stable in the slightly basic buffer and the presence of glutathione, but not as stable in the presence of the stronger biological reductant, ascorbic acid.

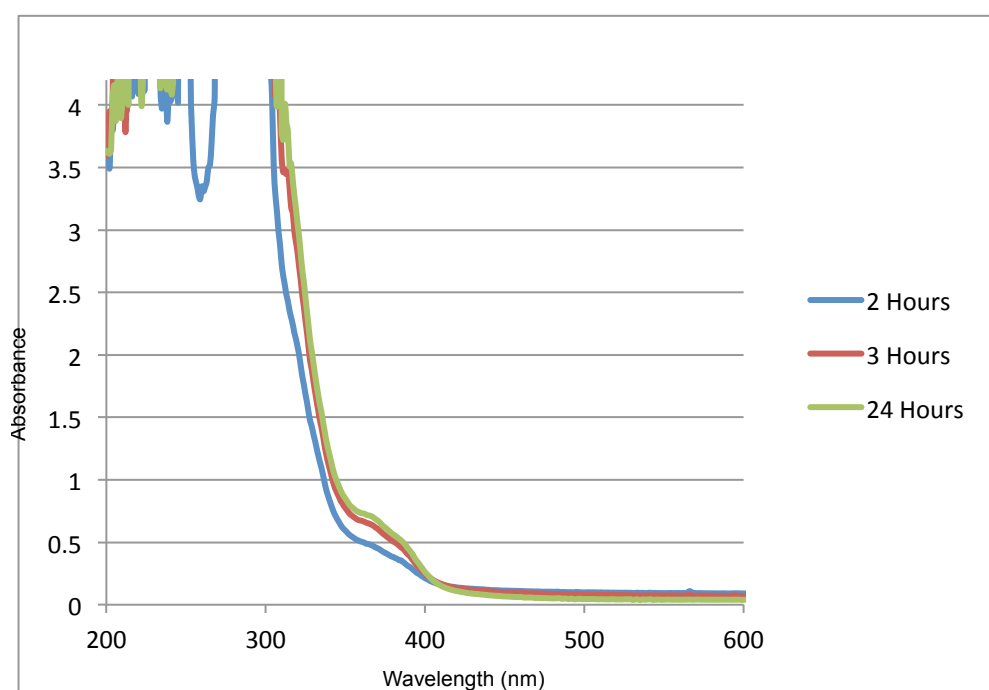


**Figure 13:** Ascorbic acid stability of 5,6-dimethyl-2,9-disecbutyl-1,10-phenanthroline gold(III) complex ( $5 \times 10^{-5}$ M) in 10 mM phosphate (pH 7.4, 20 mM NaCl,  $5 \times 10^{-5}$  M ascorbic acid) at  $37^\circ\text{C}$ . Spectra collected once every hour for 24 hours.

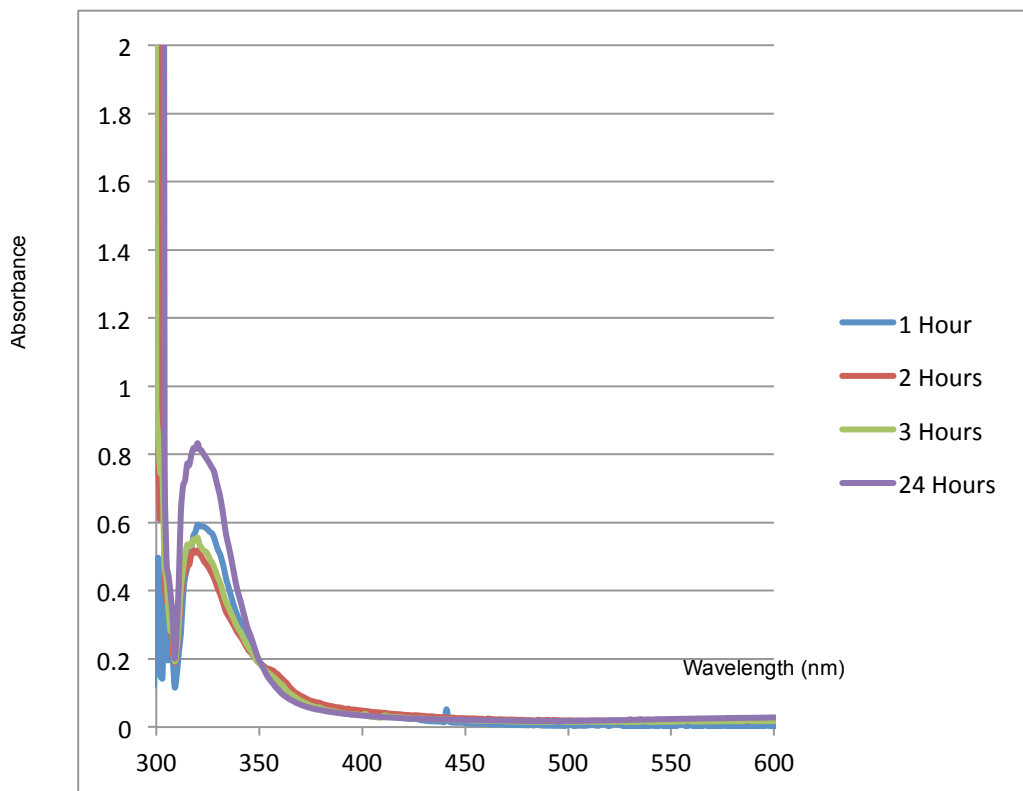


**Figure 14:** Ascorbic acid stability of 4-methyl-2,9-disecbutyl-1,10-phenanthroline gold(III) complex ( $5 \times 10^{-5}$  M) in 10 mM phosphate (pH 7.4, 20 mM NaCl,  $5 \times 10^{-5}$  M ascorbic acid) at  $37^\circ\text{C}$ . Spectra collected once every hour for 24 hours.

### *DNA Binding*

The dipyriddy oxide gold(III)'s *in vitro* DNA binding was probed with the gold complex being incubated at  $37^\circ\text{C}$  in buffer and calf thymus DNA. A control for this study consisted of the gold complex incubated in buffer, without the presence of DNA. After 24 hours of incubation, the samples were centrifuged in 10,000 MW filter tubes. The flow through of each of the tubes was studied via UV-vis analysis. The absorption data of the control was compared with the experimental DNA gold complex sample. Based off of the minimal difference of absorption of the gold peak between the control and experimental samples, the dipyriddy oxide gold(III) complex does not exhibit obvious *in vitro* DNA binding (Figure 15).

In vitro DNA binding studies were also conducted in the same manner for the 5,6-dimethyl-2,9-disecbutyl-1,10-phenanthroline gold(III) complex and the 4-methyl-2,9-disecbutyl-1,10-phenanthroline gold(III) complex. Both of these gold complexes demonstrated significant DNA binding. The spectra for compound **7** exhibited a shift in the wavelengths of the peaks, which suggests an electronic change from the initial study without the presence of DNA (Figure 16). This shift in addition to the absence of the gold(III) peak suggest that DNA binding did occur. The spectrum for the compound **9** is a little less clear (Figure 17). There was no apparent shift, however the slight gold peak that was present in the spectrum without the presence of DNA disappeared in the study with DNA.

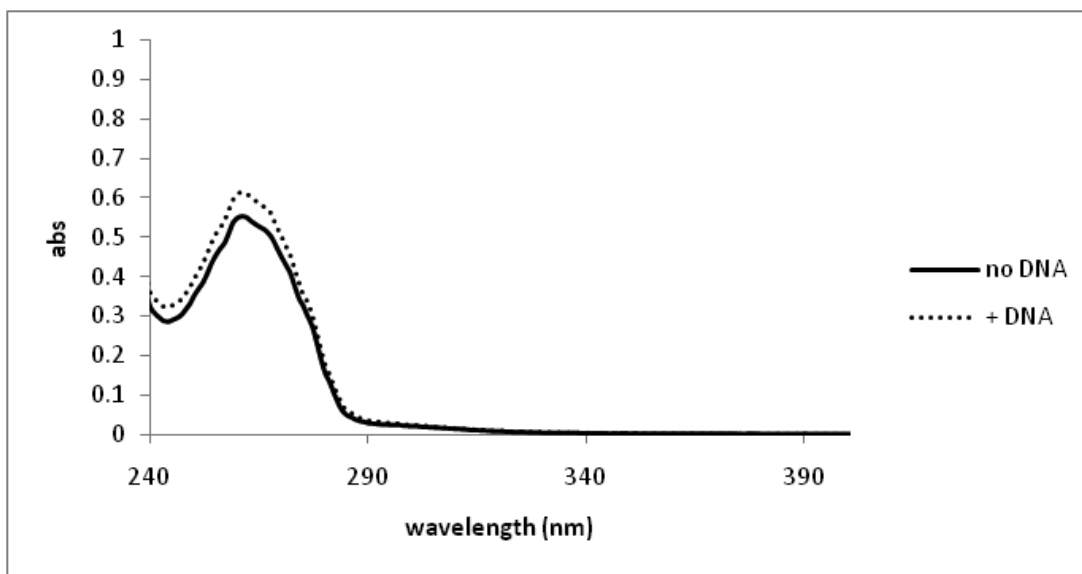


**Figure 15:** DNA binding of compound **2** ( $5 \times 10^{-5}$  M) in 10 mM phosphate (pH 7.4, 20 mM NaCl) with calf thymus DNA (10 bp/mole gold). Gold/DNA solution, and a no-DNA control with  $5 \times 10^{-5}$  M compound **2** were incubated at 37°C overnight. UV-vis spectra were collected after the solutions were passed through a 10,000 MW centrifugal filter.

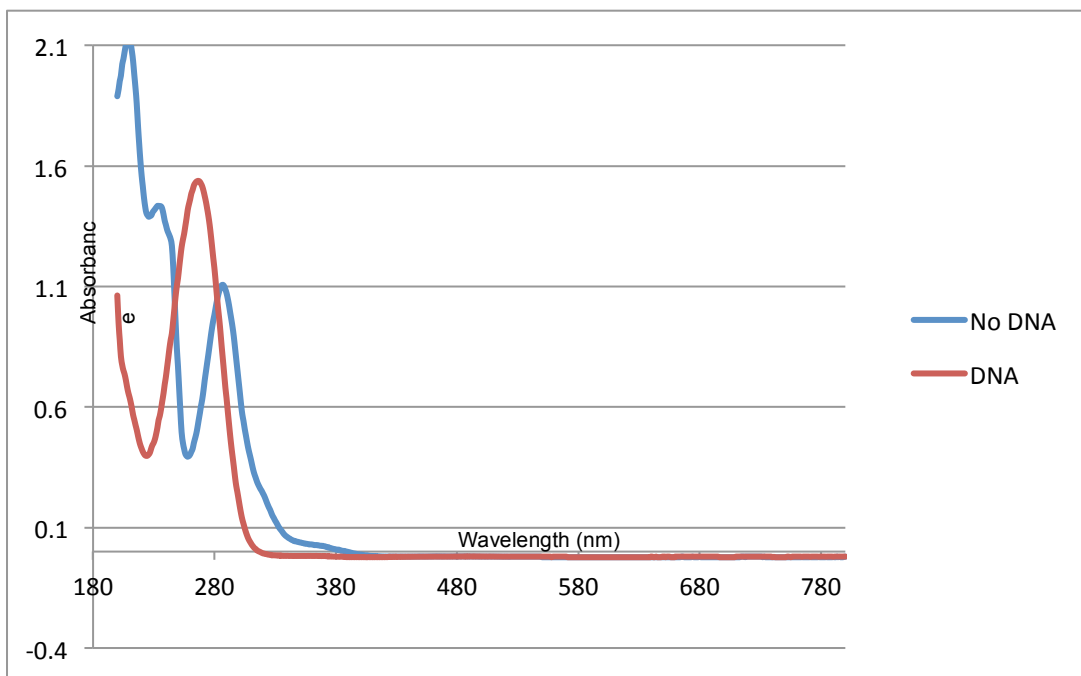


**Figure 16:** DNA binding of 5,6-dimethyl-2,9-disecbutyl-1,10-phenanthroline gold(III) complex. Gold/DNA solution, and a no-DNA control were incubated at 37°C for one hour. UV-vis spectra were collected after the solutions were passed through a 10,000 MW centrifugal filter.

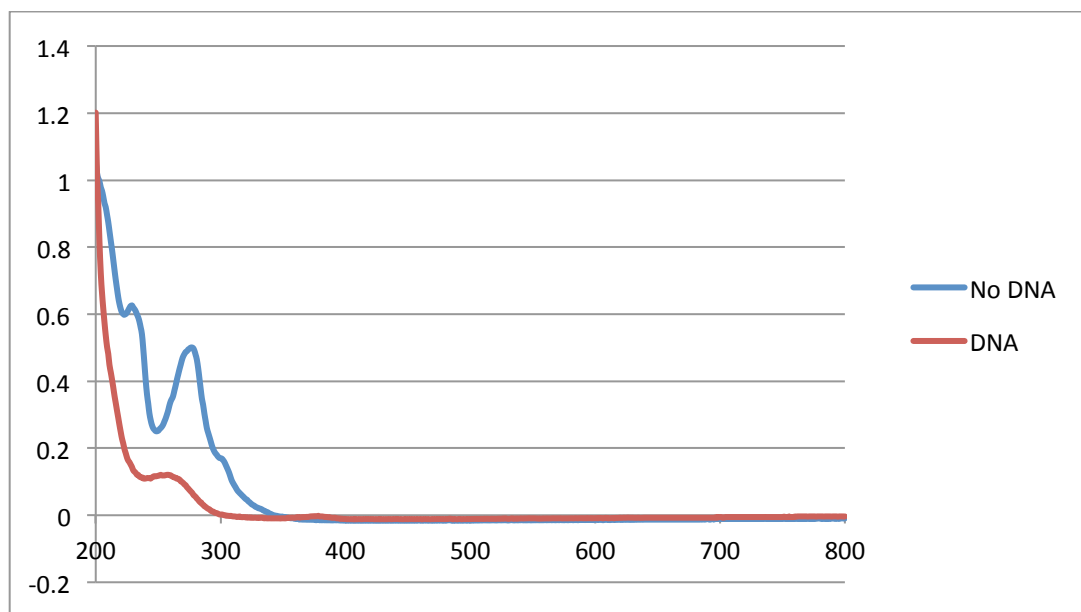


**Figure 17:** DNA binding of 4-methyl-2,9-disecbutyl-1,10-phenanthroline gold(III) complex. Gold/DNA solution, and a no-DNA control were incubated at 37°C for one hour. UV-vis spectra were collected after the solutions were passed through a 10,000 MW centrifugal filter.

### *Conclusion*

Dipyridyl sulfide gold(III), dipyridyl ketone gold(III), and dipyridyl oxide gold(III) were synthesized and characterized with X-ray crystallography. Based on the resultant X-ray crystal structures, dipyridyl oxide gold (III) complex was chosen to further evaluate with buffer stability and DNA binding studies. The monodentate dipyridyl oxide gold complex exhibited minimal DNA binding, but displayed poor stability in buffer.

After synthesizing the 5,6-dimethyl-2,9-disecbutyl-1,10-phenanthroline ligand , the 4-methyl-2,9-disecbutyl-1,10-phenanthroline ligand, the 4-methyl-2,9-disecbutyl-1,10-phenanthroline gold(III) complex, and the 5,6-dimethyl-2,9-disecbutyl-1,10-phenanthroline gold (III) complex, the two ligands were purified by column chromatography and the gold complexes were purified using recrystallization . Their purity was confirmed via NMR spectroscopy. After this confirmation, the biological properties of the two gold complexes were studied using buffer stability, GSH stability, ascorbic acid stability, and DNA binding. Both of the gold complexes demonstrated consistent stability in slightly basic buffer and the presence of glutathione. The presence of ascorbic acid caused the gold complexes to exhibit a limited stability over the 24-hour period of study. Each of the gold complexes appeared to exhibit in vitro DNA binding. Despite this in vitro DNA binding, these gold complexes may not bind to DNA in a biological system. This is because the DNA binding study is merely a basic protocol to probe whether or not the complex is able to interact with the DNA in solution; it does not determine the affinity of the complex for DNA in vitro, nor how the presence of biological reductants affect the DNA binding.<sup>39</sup> Because of these test results, in addition to the aforementioned cytotoxicity results of similar ligands produced by our lab (See table 1), these two gold complexes are potential candidates for anti-cancer therapies.

The syntheses of the 4,5,6,7-tetramethyl-2,9-disecbutyl-1,10-phenanthroline, the 5-methyl-2,9-disecbutyl-1,10-phenanthroline ligand, the 4,5,6,7-tetramethyl-2,9-disecbutyl-1,10-phenanthroline gold (III) complex, and the 5-methyl-2,9-disecbutyl-1,10-phenanthroline gold (III) complex demonstrated low yields. In addition to these low yields, the amount of purified ligand after conducting flash column chromatography was minimal, even after running these columns with different solvents. Thus, because of these low yields, these compounds did not seem to be viable options for anti-cancer therapies. Ultimately, future studies using these gold compounds or related gold complexes supported by polypyridyl chelating ligands may lead to the development of stable, non-toxic chemotherapeutic agents that are highly selective for cancerous cell lines. More studies are needed to understand and probe the mechanism of action for this specific class of gold complexes.

## References

1. Heron, M.; Tejada-Vera, B. Deaths: Preliminary Data for 2007. *National Vital Statistics Reports*, **2009**, 58.
2. Casini, A.; Ketler, G.; Gabbiana, C.; Cinellu, M. A.; Minghetti, G.; Fregona, D.; Fiebig, H. -H.; Messori, L. Chemistry, antiproliferative properties, tumor selectivity, and molecular mechanisms of novel gold (III) compounds for cancer treatment: a systematic study. *J Biol Inorg Chem*, **2009**, 14, 1139-49
3. Kostova, I. *Recent Patents on Anti-Cancer Drug Discovery*, **2006**, 1, 1.
4. Kostova, I. Gold Coordination Complexes as Anticancer Agents. *Anti-Cancer Agents Med. Chem.*, **2006**, 6, 19.
5. Hudson, Z. D.; Sanghvi, C. D.; Rhine, M. A.; Ng, J. J.; Bunge, S. D.; Hardcastle, K. I.; Saadein, M. R.; MacBeth, C. E.; Eichler, J. F. Synthesis and characterization of gold(III) complexes possessing 2,9-dialkylphenanthroline ligands: to bind or not to bind?. *Dalton Trans.*, **2009**, 7473.
6. Marcon, G.; Carotti, S.; Coronello, M.; Messori, L.; Mini, E.; Orioli, P.; Mazzei, T.; Cinellu, M. A.; Minghetti, G. Gold (III) Complexes with Bipyridyl Ligands: Solution Chemistry, Cytotoxicity, and DNA Binding Properties. *J. Med. Chem*, **2002**, 45, 1672.
7. McCann, M.; Coyle, B.; McKay, S.; McCormack, P.; Kavanagh, K.; Devereux, M.; McKee, V.; Kinsella, P.; O'Connor, R.; Clynes, M. Synthesis and X-ray crystal structure of [Ag(phendio)<sub>2</sub>]ClO<sub>4</sub> (phendio=1,10-phenanthroline-5,6-dione) and its effects on fungal and mammalian cells. *BioMetals*, **2004**, 17, 635.
8. Palanichamy, K.; Ontko, A. C. Synthesis, characterization, and aqueous chemistry of cytotoxic Au(III) polypyridyl complexes. *Inorg. Chim. Acta*, **2006**, 359, 44.
9. Shaw, C. F. Gold-based Therapeutic Agents. *Chem. Rev.*, **1999**, 99, 2589.
10. Sun, Raymond W.-Y.; Li, Carrie K.-L.; Ma, D.-L.; Yan, Jessie J.; Lok, C.N.; Leung, C.-H.; Zhu, N.; Che, C.-M. Stable Anticancer Gold(III)-Porphyrin Complexes: Effects of Porphyrin Structure. *Chem. Eur. J.*, **2010**, 16, 3097.
11. Thang, D. C.; Jacquignon, P.; Dufour, M. Synthesis of heterocyclic amines and carcinostatic potential. *J. Heterocycl. Chem.*, **1976**, 13, 641.
12. Tiekink, E. R. T. Gold derivatives for the treatment of cancer. *Crit. Rev. Oncol. Hematol.*, **2002**, 42, 225.
13. Wong, E.; Giandomenico, C. M. Current Status of Platinum-based Antitumor Drugs. *Chem. Rev.*, **1999**, 99, 2451.
14. Zhang, C. X.; Lippard, S. J. New metal complexes as potential therapeutics. *Curr. Opin. Chem. Biol.*, **2003**, 7, 481.
15. Casini, A.; Cinellu, M. A.; Minghetti, G.; Gabbiani, C.; Coronello, M.; Mini, E.; Messori, L. Structural and Solution Chemistry, Antiproliferative Effects, and DNA and Protein Binding Properties of Series of Dinuclear Gold (III) Compounds with Bipyridyl Ligands. *J. Med. Chem.*, **2006**, 49, 5524.
16. Messori, L.; Orioli, P.; Tempi, C.; Marcon, G. Interactions of Selected Gold(III) Complexes with Calf Thymus DNA. *Biochem. Biophys. Res. Commun.*, **2001**, 281, 352.
17. Coronello, M.; Marcon, G.; Carotti, S.; Caciagli, B.; Mini, E.; Mazzei, T.; Orioli, P.; Messori, L. Electrochemical behavior of cyclometalated gold(III) complexes. *Oncol. Res.*, **2001**, 12, 361.
18. Chew, E.-H.; Lu, J.; Bradshaw, T. D.; Holmgren, A. Thioredoxin reductase inhibition by



- antitumor quinols: a quinol pharmacophore effect correlating to antiproliferative activity. *FASEB J.*, **2008**, 22, 2072.
19. Rhine, M., Honors Thesis, Emory University, 2009.
  20. APEX; II ed.; Bruker AXS, Inc.: Madison, WI, 2005.
  21. SAINT; 6.45A ed.; Bruker AXS, Inc.: Madison, WI, 2003.
  22. Shaik, N.; Martinez, A.; Augustine, I.; Giovinazzo, H.; Valera-Ramirez, A.; Sanau, M.; Aguilera, R. J.; Contel, M. Synthesis for Apoptosis-Inducing Iminophosphorane Organogold(III) Complexes and Study of Their Interactions with Biomolecular Targets. *Inorg. Chem.*, **2009**, 48, 1577-1587.
  23. Bindoli, A.; Rigobello, M. P.; Scutari, G.; Gabbiana, C.; Casini, A.; Messori, L. Thioredoxin reductase: A target for gold compounds acting as potential anticancer drugs. *Coordination Chemistry Reviews*, **2009**, 253, 1692-1707.
  24. Milac, V.; Chen, D.; Ronconi, L.; Landis-Piwowar, K. R.; Fregona, D.; Dou, Q. P. A Novel Anticancer Gold(III) Dithiocarbamate Compound Inhibits the Activity of a Purified 20S Proteasome and 26S Proteasome in Human Breast Cancer Cell Cultures and Xenografts. *Cancer Res.*, **2006**, 66, 10478-10486.
  25. Milacic, V.; Dou, Q. P. The tumor proteasome as a novel target for gold(III) complexes: Implications for breast cancer therapy. *Coordination Chemistry Reviews*, **2009**, 253, 1649-1660.
  26. Abbate, F.; Driolo, P.; Bruni, B.; Marcon, G.; Messori, L. Synthetic, spectroscopic, biological, and X-ray crystallographic structural studies on a novel pyridine-nitrogen-bridged dimeric nickel(II) complex of a pentadentate N<sub>3</sub>S<sub>2</sub> ligand. *Inorg. Chim. Acta*, **2000**, 311, 1-5.
  27. Delgado, S.; Santana, A.; Castillo, O.; Zamora, F. Dynamic combinatorial chemistry in a solvothermal process of Cu(I,II) and organosulfur ligands. *Dalton Trans.*, **2010**, 39, 2280-2287.
  28. Fitchett, C.; Steel, P. Synthesis and X-ray crystal structure of dinuclear silver(I) complexes of heteroaryl thioethers. *Inorg. Chim. Acta*, **2000**, 310, 127-132.
  29. Romeo, R.; Scolaro, L.; Nastasi, N.; Arena, G. Rates of Dimethyl Sulfoxide Exchange in Monoalkyl Cationic Platinum(II) Complexes Containing Nitrogen Bidentate Ligands, A Proton NMR Study. *Inorg Chem*, **1996**, 35, 5087-5096.
  30. Sanghavi, C., Honors Thesis, Emory University, 2011.
  31. Hotchkiss, R.S.; Strasser, A.; McDunn, J.E.; Swanson, P.E. Mechanisms of Disease: Cell Death. *N. Engl. J. Med.* **2009**, 361, 1570.
  32. Rigobello, M.P.; Messori, L.; Marcon, G.; Agostina Cinellu, M.; Bragadin, M.; Folda, A.; Scutari, G.; Bindoli, A. Gold complexes inhibit mitochondrial thioredoxin reductase: consequences on mitochondrial functions. *J Inorg Biochem.* **2004**, 98, 1634.
  33. SHELXTL; 6.12 ed.; Bruker AXS, Inc: Madison, WI, 2002.
  34. International Tables for X-ray Crystallography; Wilson, A. J. C., Ed.; Kynoch Academic: Dordrecht, 1992; Vol. C.
  35. Skehan, P.; Storeng, R.; Scudiero, D.; Monks, A.; McMahon, J.; Vistica, D.; Warren, J. T.; Bokesch, H.; Kenney, S.; Boyd, M. R. J. New Colorimetric Cytotoxicity Assay for Anticancer-Drug Screening. *Natl. Cancer Inst.*, **1990**, 82, 1107.
  36. Boduszek, B.; Wieczorek, J. Synthesis of Dipyrindyl Sulfides from Pyridyl-Pyridinium Halides. *Chemical Monthly*, **1980**, 1111-1116.

37. Segapelo, T.; Guzel, I.; Spencer, L.; Zyl, W.; Darkwa, J. (Pyrazolylmethyl)pyridine platinum(II) and gold(III) complexes: Synthesis, structures, and evaluation as anticancer agents. *Inorg. Chim. Acta*, **2009**, 362, 3314-3324.
38. Casini, A.; Diawara, M.; Scopelliti, R.; Zakeeruddin, S.; Gratzel, M.; Dyson, P. Synthesis, characterization, and biological properties of gold(III) compounds with modified bipyridine and bipyridylamine ligands. *Dalton Transactions*, **2010**, 39, 2239-2245
39. Arakawa, H.; Ahmad, R.; Naoui, M.; Tajmir-Riahi, H.A. A comparative study of calf thymus DNA binding to Cr(III) and Cr(VI) ions. Evidence for the guanine N-7-chromium-phosphate chelate formation. *J. Biol. Chem.* **2000**, 275, 10150.